JASON

Technical Report JSR-74-3 *March 1975*

A COMPUTER CODE TO CALCULATE THE EFFECT OF INTERNAL WAVES ON ACOUSTIC PROPAGATION

By: STANLEY M. FLATTÉ FREDERICK D. TAPPERT

Contract No. DAHC15-73-C-0370
ARPA Order No. 2504
Program Code No. 3K10
Date of Contract: 2 April 1973
Contract Expiration Date: 30 June 1976
Amount of Contract: $2,062,014

Sponsored by

DEFENSE ADVANCED RESEARCH PROJECTS AGENCY
ARPA ORDER NO. 2504

STANFORD RESEARCH INSTITUTE
Menlo Park, California 94025 · U.S.A.

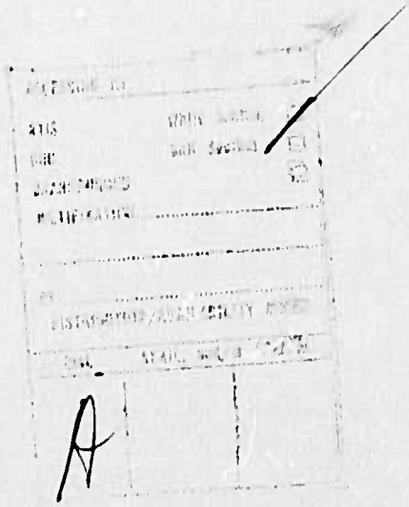

SECURITY CLASSIFICATION OF THIS PAGE (When Data Entered)

REPORT DOCUMENTATION PAGE

READ INSTRUCTIONS BEFORE COMPLETING FORM

1. REPORT NUMBER: JRS-74-3 (14) SRI
2. GOVT ACCESSION NO.
3. RECIPIENT'S CATALOG NUMBER

4. TITLE (and Subtitle): (6) A COMPUTER CODE TO CALCULATE THE EFFECT OF INTERNAL WAVES ON ACOUSTIC PROPAGATION

5. TYPE OF REPORT & PERIOD COVERED: (7) Technical Report

6. PERFORMING ORG. REPORT NUMBER: SRI [redacted]-3000

7. AUTHOR(s): (10) Stanley M. Flatté and Frederick D. Tappert

8. CONTRACT OR GRANT NUMBER(s): (15) DAHC15-73-C-0370, ARPA Order-2511

9. PERFORMING ORGANIZATION NAME AND ADDRESS
Stanford Research Institute
Menlo Park, California 94025

10. PROGRAM ELEMENT, PROJECT, TASK AREA & WORK UNIT NUMBERS: (11) NR 75 (12) 62p.

11. CONTROLLING OFFICE NAME AND ADDRESS
Defense Advanced Research Projects Agency
1400 Wilson Boulevard
Arlington, Virginia 22209

12. REPORT DATE: June 1975
13. NO. OF PAGES: 80

14. MONITORING AGENCY NAME & ADDRESS (if diff. from Controlling Office)

15. SECURITY CLASS. (of this report): UNCLASSIFIED

15e. DECLASSIFICATION/DOWNGRADING SCHEDULE

16. DISTRIBUTION STATEMENT (of this report)

Approved for public release; distribution unlimited.

17. DISTRIBUTION STATEMENT (of the abstract entered in Block 20, if different from report)

18. SUPPLEMENTARY NOTES

19. KEY WORDS (Continue on reverse side if necessary and identify by block number)

Ocean acoustics
Acoustic propagation
Acoustic fluctuations
Internal waves
Computer simulation
Vertical arrays

20. ABSTRACT (Continue on reverse side if necessary and identify by block number)

The signal received by a hydrophone in the ocean many kilometers from a steady sound source fluctuates dramatically due to variations of the speed of sound in sea-water. ~~We have written~~ a computer code that simulates the passage of acoustic CW signals through an ocean with internal waves. is written The code generates a sound-speed field from an internal-wave spectrum that has been derived from oceanographic measurements. The acoustic propagation is achieved through the use of the parabolic-equation approximation. The code is limited fundamentally to acoustic

→ over

DD FORM 1 JAN 73 1473
EDITION OF 1 NOV 65 IS OBSOLETE

SECURITY CLASSIFICATION OF THIS PAGE (When Data Entered)

330500

4/8

19. KEY WORDS (Continued)

20 ABSTRACT (Continued)

frequencies above ~~≈~~ approx 10 Hz, and by practical computer-time constraints to frequencies below ≈ 400 Hz. The code allows the calculation of the amplitude and phase of the full acoustic field as a function of depth and range at any desired time.

CONTENTS

LIST OF ILLUSTRATIONS

LIST OF TABLES

I INTRODUCTION

Sonar has been used for detection and communication in the ocean for many years. The effect on sonar of a geographical variation in the sound-speed profile of the ocean has received considerable attention as more precise and sensitive use has been made of acoustic signals in the ocean. However, relatively little attention has been focused on the smaller-scale variations in the oceans--in particular, the internal waves, which not only provide variations in space (on scales of a few hundred meters vertically and a few kilometers horizontally), but also introduce the new dimension of time variability (on a scale of a few hours).

The theory of sound propagation through internal waves has not yet been fully developed, so that many questions of a qualitative nature are open. We have written a computer code to answer some of these questions, taking advantage of the advent of the use of the parabolic equation method in underwater acoustics,[1-3*] and the existence of internal-wave models derived from oceanographic measurements.[4] With certain restrictions (to be described) the full acoustic-wave field can be propagated through an ocean with variable sound speed, and the resulting long-range transmission characteristics can be studied.

---

*References are listed at the end of the report.

Consider the acoustic pressure in the ocean as $p(\vec{r},t)$. The wave equation for p is

$$\nabla^2 p - \frac{1}{c^2}\frac{\partial^2 p}{\partial t^2} = 0 \quad ,$$

where it has been assumed that the sound speed $c(\vec{r},t)$ varies slowly with position and that the water density, as far as its effect on inertia is concerned, is essentially constant. Hence, the quantity that determines the structure and behavior of the pressure is the sound speed $c(\vec{r},t)$.

In the following sections we present a model for the expected sound-speed structure in the ocean, the parabolic equation approximation to the wave equation and the reasons it is valid for our model of the sound-speed structure, and the computer code that has combined the model of internal waves and the parabolic equation method into a useful apparatus for studying oceanic sound transmission.

Initial results obtained through use of our code are given in Reference 6.

II OCEAN SOUND-SPEED STRUCTURE

A. Deterministic Profile

On the scale of the depth of the ocean (4 to 5 km) the sound speed as a function of depth, z, is determined by the gross behavior of the density, temperature, and salinity. We use the profile derived by Munk,[5] whose input is an exponentially decreasing density gradient. The resulting "canonical" profile is

$$c_{CP}(z) = c_1 \left\{ 1 + \epsilon \left[e^{-\eta} - (1-\eta) \right] \right\}$$

where $\eta = \frac{z-z_A}{\frac{1}{2}B}$.

Note that c(z) has a minimum at z_A, that the width of the minimum is B, and that the deviation of the sound speed from the minimum value c_1 is of order ϵ.

Typical (though not universal) values for the parameters are:

$z_A = 1300$ m

$B = 1300$ m

$\epsilon = 0.74 \times 10^{-2}$

$c_1 = 1500$ m/s

See Figure 1* for a graph of $c_{CP}(z)$ using these parameters.

---

*Illustrations are grouped at the end of the report.

One must point out that realistic ocean profiles in most cases have significantly different behavior from this general form. For example, within a few hundred meters of the surface a mixed layer usually results in a lowered sound-speed gradient. However, we ignore these details in the present version of the code.

B. Internal Waves

The density gradient in the ocean leads to the possibility of waves traversing the volume of the ocean just as the density discontinuity at the surface leads to the possibility of surface waves. The density gradient is usually presented in the form

$$N(z) \equiv \left\{ -\frac{g}{\rho_o} \frac{\partial \rho}{\partial z} \right\}^{1/2}$$

where N(z) is called the local stability (Brunt-Väisälä) frequency.

Munk's model for N(z) is

$$N(z) = n_o e^{-z/B}$$

where n_o = 4 cycles/hr.

Let $w(\vec{r},t)$ be the displacement of a particular density level from its mean position. It can be shown that w satisfies the equation:

$$\frac{\partial^2}{\partial t^2}\left(\nabla^2 w\right) + N^2(z)\nabla_h^2 w = 0 \quad .$$

The eigenmodes of this equation can be found by taking

$$w = W(j,k,z)e^{i[k_1 x + k_2 y - \omega(j,k)t]}$$

where $k = \sqrt{k_1^2 + k_2^2}$ = horizontal wave number.

Substituting, we have

$$W'' + \frac{N^2(z) - \omega^2}{\omega^2} k^2 W = 0$$

Modifying this equation to account for the rotation of the earth we find

$$W'' + \left(\frac{N^2(z) - \omega^2}{\omega^2 - \omega_i^2} \right) k^2 W = 0$$

where ω_i = inertial frequency = (2 cycles/day)sin(latitude).

Boundary conditions are $W(z) = 0$ at surface and bottom. Thus, for a given horizontal wave number there are a discrete infinity of solutions to this equation labeled by the mode number j, with frequencies $\omega(j,k)$. The sound-speed fluctuation profiles caused by each internal wave will follow the depth structure of $N^2(z)W(j,k,z)$. Several examples of such profiles are shown in Figure 2.

The sound velocity fluctuations caused by a full internal-wave field will be

$$\delta c_{IW} = \mathrm{Re} \left\{ \sum_{j,k_1,k_2} B(j,k_1,k_2) e^{i[k_1 x + k_2 y - \omega(j,k)t]} N^2(z) W(j,k,z) \right\} .$$

The difficulty of integrating this distribution over the x-z plane (because we will propagate sound only in the x-z plane with the acoustic transmission code) has caused us to consider a simplified version of the internal-wave spectrum where internal waves are propagated only in (or opposite to) the direction that the sound waves propagate. In addition,

we combine real and imaginary parts to reduce fluctuations in the overall energy in the internal waves as a function of time:

$$\delta c_{1W} = \frac{c_1}{\sqrt{2}} \left\{ \text{Re } \Delta + \text{Im } \Delta \right\}$$

$$\Delta = \sum_{j,k} A(j,k)\ W(j,k,z) N^2(z)\ e^{i[kr-\omega(j,k)t]}$$

where $W(j,k,z)$ is normalized so that $\int_o^{z_{max}} N^4(z) W^2(j,k,z)\, dz = 1$.

The $A(j,k)$ are complex Gaussian random variables. From a synopsis of diverse oceanographic measurements, Garrett and Munk[4] have proposed the following model:

$$\langle A(j,k) A^*(j',k') \rangle = \delta_{jj'} \delta_{kk'} \frac{2\pi}{3L} \left[\left\langle \left(\frac{\delta c}{c} \right)^2 \right\rangle \Bigg|_{z=0} \right]$$

$$\cdot \frac{4\omega_i k^2 j(\alpha-1)(j_*)^{\alpha-1}}{n_o (j+j_*)^{\alpha} \left[k^2 + \left(\frac{\pi \omega_i j}{n_o B} \right)^2 \right]^2}$$

$$\left\langle \left(\frac{\delta c}{c} \right)^2 \right\rangle \Bigg|_{z=0} = \left(4 \times 10^{-4} \right)^2$$

where $j_* = 3$, $\alpha = 2.5$, and L is the horizontal periodicity length over which the internal waves are generated (because we are generating k in discrete steps rather than as a continuum). The relative intensity of the various modes is shown in Figure 3.

Note that the magnitude of the sound-speed fluctuation due to internal waves is $\delta c/c \sim 10^{-4}$, a factor of one hundred below the magnitude of the deterministic structure. Also the spatial behavior of the sound-speed variations due to internal waves is of the order of a few hundred meters vertically and several kilometers horizontally. Internal-wave frequencies vary from $n_o = 4$ cycles/hr for the lowest mode to one cycle/day for the high modes ($j \sim 20$). Figure 4 shows some typical sound-speed profiles due to internal waves.

C. Final Expression for Sound-Speed Structure

The sound speed as a function of position and time is given by

$$c(\vec{r},t) = c_{CP}(z) + \delta c_{IW}$$

$$= c_1\left(1 + \frac{\delta c}{c}\right)$$

where

$$\frac{\delta c}{c} \equiv \underbrace{\varepsilon\left[e^{-\eta} - (1-\eta)\right]}_{O(10^{-2})} + \underbrace{\frac{\delta c_{IW}}{c_1}}_{O(10^{-4})}$$

Hence, the deviation in sound speed from a constant value is always small, and we may write, for example,

$$\frac{1}{c^2} = \frac{1}{(c_1)^2}\left\{1 - \frac{2\delta c}{c}\right\} .$$

This expression will of course appear in the wave equation.

III THE PARABOLIC-EQUATION METHOD

A. Introduction

The parabolic-equation method was originally developed by Leontovich and Fok in 1946 to study long-range propagation of radio waves in the troposphere.[1] This method was introduced into the field of underwater acoustics by Tappert in 1972, and a computer program based on this method was developed by Tappert and Hardin to solve acoustic propagation problems of interest to the Navy.[2,3]

B. Approximations and Ranges of Validity

The wave equation for acoustic pressure $p(\vec{r},t)$ is

$$\nabla^2 p - \frac{1}{c^2}\frac{\partial^2 p}{\partial t^2} = 0 \quad .$$

Since the time variation of c takes place over hours, and the acoustic frequencies will be in the range of $\sim$ 200 Hz, we may treat sound propagation at any time as though the ocean structure were frozen.

Hence, a particular acoustic frequency ω would be unaffected by the ocean and we may set

$$p = p' e^{-i\omega t}$$

$$\Rightarrow \nabla^2 p' + k^2 p' = 0 \qquad \text{where } k \equiv \frac{\omega}{c}.$$

$$\text{but } k^2 = \frac{\omega^2}{c_1^2}\left(1 - \frac{2\delta c}{c}\right) = k_o^2\left(1 - \frac{2\delta c}{c}\right)$$

$$\Rightarrow \nabla^2 p' + k_o^2 p' - 2k_o^2 \frac{\delta c}{c} p' = 0 .$$

Neglecting the $\delta c/c$ term initially, the solution in cylindrical coordinates is

$$p' \propto H_o(k_o r) \approx \frac{e^{ik_o r}}{\sqrt{r}}$$

so we try for the full solution:

$$p' = \psi_t(r,z,\varphi) H_o(k_o r)$$

where the reduced wave function ψ is labeled by the time t, because the $\delta c/c$ structure of the ocean is different for different times. Substituting p' in the full equation we find:

$$H_o \nabla^2 \Psi + \Psi \nabla^2 H_o + 2 \frac{\partial H_o}{\partial r} \frac{\partial \Psi}{\partial r} + k_o^2 H_o \Psi - 2k_o^2 \frac{\delta c}{c} H_o \Psi = 0$$

If $k_o r \gg 1$,

$$\frac{\partial H_o}{\partial r} = ik_o\left(1 - \frac{1}{2ik_o r} + O\frac{1}{k_o^2 r^2}\right) H_o$$

$$\Rightarrow \nabla^2 \Psi - \frac{1}{r}\frac{\partial \Psi}{\partial r} + 2ik_o \frac{\partial \Psi}{\partial r} - 2k_o^2 \frac{\delta c}{c} \Psi = 0$$

$$\frac{\partial^2 \Psi}{\partial r^2} + \frac{1}{r^2}\frac{\partial^2 \Psi}{\partial \varphi^2} + \frac{\partial^2 \Psi}{\partial z^2} + 2ik_o \frac{\partial \Psi}{\partial r} - 2k_o^2 \frac{\delta c}{c} \Psi = 0 .$$

The key to the parabolic-equation method involves the following physical approximations, based on the structure of $\delta c/c$:

- $k_o r \gg 1$

- $\frac{\partial^2 \psi}{\partial r^2} \ll 2ik_o \frac{\partial \psi}{\partial r}$

Valid if the objects off which the acoustic waves are scattering have sizes that are much larger than a wavelength. This is equivalent to having only relatively forward scattering, which results in small changes in ψ over an acoustic wavelength. Let L_v be the vertical scale of sound speed variations. Then $k_o L_v \gg 1$ is required. Note that energy scattered at large angles is removed by the ocean bottom anyway.

- $\frac{\partial^2 \psi}{\partial r^2} \approx \frac{1}{r^2} \frac{\partial^2 \psi}{\partial \varphi^2} \ll \frac{\partial^2 \psi}{\partial z^2}$

This is true because the canonical profile, which is 100 times larger than the sound-speed fluctuation of the internal waves, affects the z coordinate only. More importantly, however, the internal-wave gradients in the vertical are an order of magnitude greater than the horizontal.

The approximate wave equation is therefore

$$-\frac{1}{2k_o} \frac{\partial^2 \psi}{\partial z^2} + k_o \frac{\delta c}{c} \psi = i \frac{\partial \psi}{\partial r} . \qquad (1)$$

To summarize the approximations required for this parabolic equation to be valid, we need the following quantities:

ω_{IW} = Largest frequency involved in the internal-wave spectrum
$\approx$ 4 cycles/hr

L_H = Minimum horizontal scale of sound-speed fluctuations
$\approx$ 1 km

L_V = Minimum vertical scale of sound-speed fluctuations

$\approx$ 200 m.

Validity of the parabolic equation requires:

(1) $\omega \gg \omega_{IW}$

(2) $k_o r \gg 1$

(3) $L_H \gg L_V$

(4) $k_o L_V \gg 1$.

Requirement 3 is well satisfied by our internal-wave model. Requirement 4 sets a lower limit on the frequency we can treat:

$$\text{freq} \gg \frac{1}{2\pi} \frac{c_1}{L_V} \approx 1 \text{ Hz} \quad .$$

Requirement 1 is subservient to Requirement 4. Requirement 2 sets a lower limit on the range of sound transmission:

$$R \gg \frac{1}{k_o} \approx 25 \text{ m for 10 Hz} \quad .$$

Thus, any experiments with frequencies of 10 Hz or higher over ranges of $(10)/k_o$ or longer should be well treated by the parabolic equation. This includes all problems of interest at present.

C. Analogy with Quantum Mechanics

The Schrödinger equation in nonrelativistic quantum mechanics is

$$-\frac{1}{2m}\frac{\partial^2 \psi}{\partial z^2} + V(z)\psi = i\frac{\partial \psi}{\partial t} \quad . \tag{2}$$

We see that our parabolic equation (1) is of the same form if the analogies are made as follows:

Mass = k_o

Potential = $k_o \frac{\delta c}{c}$

Time = range

Energy level = horizontal wave number

Momentum = angle $\left(\frac{dz}{dr}\right)$.

Many characteristics of underwater acoustics can be easily understood on the basis of this analogy. We will give two examples for transmission with $\delta c/c$ given by the canonical profile (no internal waves):

(1) Rays--Consider a narrow wave packet with velocity v propagating in our potential well [see Figure 5(b)]. As long as $\frac{1}{2}mv^2 < V_{max}$ the packet will bounce back and forth inside the well. The analogy says that as long as $\frac{1}{2}k_o\theta \ll k_o\,(\delta c/c)_{max}$, a ray starting from the sound axis with θ will be contained within the sound channel [see Figure 5(a)].

(2) Ground State--Forming a wave packet with the form $\psi_o(z)$ where ψ_o is the ground-state wave function of the potential V(z) would result in an acoustic field propagating in range with no change in structure--i.e., no spreading of the wave packet (see Figure 6).

IV NUMERICAL REALIZATION OF THE INTERNAL-WAVE MODEL

A. Eigenfunction Determination

A program (ZMODE)[7] was used to numerically generate the eigenfunctions $W(j,k,z)$ and frequencies $\omega(j,k)$. Several modifications to ZMODE were required:

(1) An increase of dimensions so that 128 values of k and 256 values of z can be treated.

(2) Inclusion of the inertial frequency ω_i.

(3) Change of the initial guess for $\omega(j,k)$. $\gamma_m(0) = (m-\frac{1}{4})\pi$ instead of $(m-\frac{1}{2})\pi$.

B. Range of j and k

Modes with $1 \leq j \leq 24$ are included. Values of k range from $(k_{max}/128)$ to $(127/128)k_{max}$ in 127 equal steps. Both positive and negative values of k are included, making a total of 254 values of k. The value of k_{max} is 1 cycle/km at present. Thus a total of 254 x 24, or 6096 separate modes, are generated.

C. Generation of δc_{IW}

The steps in generating the sound-speed deviations caused by internal waves, δc_{IW}, are as follows:

(1) The 6096 different A(j,k) are generated according to a Rayleigh probability distribution in amplitude, and

variance given by the spectrum described in Section II. The phase angle of each A(j,k) is randomly generated in the region 0 to 2π. Thus, 12192 random numbers are needed.

(2) For each j value, the values of k are stepped through, calculation of the function W(j,k,z) is accomplished, and a matrix element is incremented until the following complex matrix is completed:

$$M(k,z) = \sum_j A(j,k)N^2(z)W(j,k,z)e^{i\omega(j,k)t} .$$

(3) The value of δc_{IW} at range r and depth z is the Fourier transform of M(k,z): $\Delta(r,z) = \sum M(k,z)e^{ikr}$. The matrix Δ is calculated from M by the fast-Fourier-transform technique. The values of r at which Δ is known are $0 < r \leq 256\pi/k_{max}$ in steps of π/k_{max}. In the present code this means $0 < r \leq 128$ km; the code simply repeats the structure it has, every 128 km.

We repeat that

$$\delta c_{IW} = \frac{c_1}{2} [Re\Delta + Im\Delta] .$$

Hence we have the internal-wave sound-speed deviations at time t on a grid of 128 km by 4 km with 256 points horizontally and 256 points vertically. (Step size $\sim$ 16 m vertically and 0.5 km horizontally.)

(4) The propagation section of the code may need the value of δc_{IW} on points off the above grid. The code allows division of the grid into a finer grid by powers of two, with the values of δc_{IW} on the fine grid being obtained by cubic spline interpolation (see Appendix).

(5) The 256 × 256 grid of δc_{IW} values is kept in Large Core memory for fast access during the sound-propagation phase of the code. When the values of δc_{IW} at a new time t are desired, the entire procedure is repeated with a new time t, with two exceptions; first, the random numbers do not need to be generated again, and second, the eigenvalues $\omega(j,k)$ do not need to be calculated again because they have been saved in computer memory. Due to storage limitations, however, the functions $W(j,k,z)$ must be recalculated at every t, since they have not been saved.

V NUMERICAL PROPAGATION OF THE ACOUSTIC FIELD USING THE PARABOLIC EQUATION

A. Algorithm

We must numerically solve the parabolic equation

$$\frac{\partial \Psi}{\partial r} = \frac{1}{2k_o}\frac{\partial^2}{\partial z^2} - ik_o\frac{\delta c}{c}\Psi = i(A + B)\Psi$$

where reference to the variable z is suppressed, and where A and B are real operators. The first-order solution, useful for a numerical method, is:

$$\Psi(r+dr) = e^{iA\frac{dr}{2}} e^{iBdr} e^{iA\frac{dr}{2}} \Psi(r) \quad .$$

Since step follows step, we use

$$\Psi(r + dr) = e^{iAdr} e^{iBdr} \Psi(r) \quad .$$

Evaluation of e^{iBdr} is straightforward--it is a complex number with unit modulus. Evaluation of e^{iAdr} is more complicated since A is a differential operator:

$$e^{iAdr}\phi(z) = F^{-1} e^{i\hat{A}dr} F[\phi(z)] \quad .$$

F is a fast-Fourier-transform operation, and

$$\hat{A} = -\frac{i}{2k_o}k^2$$

in k-space.

This algorithm is fast, and also it is very stable, since the total acoustic energy

$$\int |\psi|^2 dz$$

is exactly conserved as a function of r. This is because the operations on $\psi(r)$ are exactly unitary.

B. Acoustic Source

The acoustic field may be started with any function of depth. The present code models a point source, at a depth provided as input, with unit strength at 1 yard.

C. Surface Boundary Condition

The reduced wave function ψ must be exactly zero at the ocean surface (pressure release boundary condition). In order to ensure the proper application of this condition, a "reflected ocean" is carried along with the real ocean. In the reflected ocean is an image source of the same strength as the real source, but reflected in position and 180° out of phase with the real source (see Figure 7).

D. Bottom Absorption

In order to avoid reflection off the ocean bottom, a gradual loss of intensity is imposed on $\psi(z)$ as z nears the ocean bottom. The functional form of the imposed loss is

$$\psi(r+dr) = L(z) e^{iAdr} e^{iBdr} \psi(r)$$

$$L(z) = \exp\left\{ -\alpha\, dr\, e^{-\left(\frac{z-z_{max}}{\beta}\right)^2} \right\} .$$

The code has at present

$$\alpha = 0.05/m$$

$$\theta = 0.04\ z_{max} \quad .$$

This form effectively stops any acoustic energy from penetrating below about 500 m above the bottom. Even this form does cause some reflection off the bottom at a low-intensity level, for long-wavelength sound.

E. Number of Depth Points

The maximum number of depth points in the real ocean allowed by the code is 1024 (the number used must be a power of two).

F. Size of Range Step

The size of the range step should not be too large or the numerical algorithm will break down. Experience has indicated that 0.5 km is a safe step at 100 Hz and 0.25 km is safe at 400 Hz.

VI FORMAT OF SAVED DATA FROM COMPUTER RUNS

As the sound-propagation code is run, various quantities are put on magnetic tape, much in the manner of an actual field experiment. The tapes can then be separately analyzed.

At the present the output consists of the following logical records:

(1) An identification record (see Table 1).

(2) A number of data records containing the acoustic field at various points (see Table 2). For each time step the full acoustic field is output for 12 values of the range, and the acousric field at four selected depths is output for all values of the range.

(3) An end-of-file mark.

Table 1

IDENTIFICATION RECORD

Word Number	Quantity	Format
1	Number of words following	I
2	Frequency (Hz)	F
3	c_1 (m/s)	F
4	z_{max} (m)	F
5	GW (m)	F
6	FGW (m)	F
7	dr (m)	F
8	k_o (m^{-1})	F
9	dz (m)	F
10	λ (m)	F
11	π	F
12	Source depth (m)	F
13	Number of depth points	I
14	$\log_2 N$	I
15	-	
16	-	
17	-	
18	c_1 (m/s)	F
19	z_A (m)	F
20	B (m)	F
21	g (s^{-1})	F
22	N_o (s^{-1})	F
23	ω_i (s^{-1})	F
24	-	F
25	z_{max}	F

Table 1 (Concluded)

Word Number	Quantity	Format
26	NZ (internal waves)	I
27	k_{max}	F
28	NK (internal waves)	I
29	NMODE (internal waves)	I
30	$[\langle(\delta c/c)^2\rangle\|_{z=0}]^{\frac{1}{2}}$	F
31	TIW	F
32	j_*	I
33	Number of range steps	I
34	Number of time steps	I
35	-	
36	Time-step interval	F

Table 2

DATA RECORD

Word	Quantity
1	Number of following words
2	r (m)
3	t (s)
4 - 1027	$\mathrm{Re}\{\psi(z_i)\}$ starting from ocean surface
1028 - 2051	$\mathrm{Im}\{\psi(z_i)\}$ starting from ocean surface
2052 - end	$\mathrm{Re}\psi(z_a,r_1)$, $\mathrm{Im}\psi(z_a,r_1)$, $\mathrm{Re}\psi(z_a,r_2)$, $\mathrm{Im}\psi(z_a,r_2)$... until all ranges since the last tape output are included for selected depth z_a. Then the same list for selected depths z_b, z_c, and z_d. (Maximum number of range steps between tape outputs is set at 100.)

VII COMPUTER RUNNING TIMES

The breakdown of the CDC 7600 computer time to run the code is as follows:

(1) To generate the δC_{IW} on a 256 × 256 grid for <u>each</u> time: 28 CPU seconds.

(2) To step the acoustic field <u>once</u> in range $0.13(N \log_2 N)'/(10 \times 1024)$ CPU seconds where N is the number of depth points at which the acoustic field is evaluated.

Hence the total running time is

$$T = NT[28 + 1.3 \times 10^{-5}(N \log_2 N)NR] \text{ CPU seconds}$$

where

NT = Number of time steps

N = Number of depth points

NR = Number of range steps at each time.

<u>Note</u>: As of September 1974 the code has been changed to make use of a fast sine transform, and the eigenfunctions W(j,k,z) are being saved on disk. This has resulted in a factor-of-two increase in speed.

VIII CODE ORGANIZATION AND LISTING

Figure 8 illustrates the program flow and the FORTRAN listing of the code in its present form is given in the following pages.

```
      PROGRAM USER(OUTPUT,TAPE6=OUTPUT,TAPE10)
      COMMON C(30)
      DIMENSION IC(30)
      EQUIVALENCE(C,IC)
      DIMENSION DPR(8),DBT(8)
      COMMON/NFACTS/N,LN,NR,NTLOSS,NIT
      COMMON/AFACTS/FREQ,SNORM,ZMAX,GW,FGW,DR,FKR,DZ,WL,PI,GD
      COMMON/VAR/R,IR,T,IT
      COMMON/ACOUST/UR(2048),UI(2048)
      COMMON/STOP/ISTOP
      COMMON/PHASES/SK(1024),CK(1024),SM(1024),CM(1024)
      COMMON/BFUR/URB(1024),UIB(1024),ANGB(1024)
      COMMON/MUNK/CA,ZA,ZW,GEE
      COMMON/IWAVES/END,FINER,BZ,EZMAX,NZ,AKMAX,NK,NMODE,DELC,
     * TIW,JSTAR
      COMMON/SAV/SAVR(100,4),SAVI(100,4)
      COMMON/STEP/NSTEP,ISTEP,NSAV,DT
      DIMENSION LR(12),LZ(4)
      DATA LR/20,40,60,80,100,120,160,200,250,320,400,500/
      DATA LZ/25,102,166,256/
      DATA END,FINER,NZ,AKMAX,NK,NMODE,DELC,TIW,JSTAR/
     * 4.,0.04,257,1.0,128,24,0.0,2.5,6/
      DATA T,IT/0.,1/
      DATA CA,ZA,ZW,GEE/1500.,1300.,1300.,0.017/
      DATA ISTOP/0/
      DATA FREQ,GD,DPR,SNORM/100.,1300.,1000.,7*0.,1500./
      DATA N,DRKM,NR,NTLOSS,ZMAX,FGW /512,.25,200,1,4000.,1./
      DATA NBF /1/
      DATA R,RKM /2*0./
      DATA PI /3.1415926356/
      R=0.
      ZBF=1300.
      IR=1
      GO TO 60
   70 CONTINUE
      CALL TAPEIW(1)
      DO 50 IT=1,ISTEP
      MR=1
      NSAV=0
      R=0.
      NP=0
      T=DT*(IT-1)
      CALL INIT
      CALL PHASE1
      CALL PHASE2
      DO 10 IR=1,NSTEP
      JR=MOD(IR,40)
      IF (DELC.EQ.0.) GO TO 767
      CALL PHASE2
  767 CONTINUE
      CALL UWS
      R=R+DR
      IF (MOD(IR,20).EQ.0) CALL PRINTP(UR,UI,N,R)
      NSAV=NSAV+1
      DO 14 IDE=1,4
      IDP=LZ(IDE)
      SAVR(NSAV,IDE)=UR(IDP)
```

```
 14 SAVI(NSAV,IDE)=UI(IDP)
    IF (IR.NE.LR(MR)) GO TO 12
    MR=MR+1
    CALL TAPEIW(2)
    NSAV=0
 12 CONTINUE
 10 CONTINUE
 50 CONTINUE
    WRITE(6,200)
    ISTOP=1
    CALL TAPEIW(3)
    STOP
 60 CONTINUE
    NSTEP=500
    FREQ=100. $  N=512
    DRKM=0.5
    DT = 3840.
    NSAV=0
    DELC=.0004
    ISTEP=32
    BZ=ZW $ EZMAX=ZMAX
    TPI=2.*PI
    END=END*TPI/3600.
    FINER=FINER*TPI/3600.
    AKMAX=AKMAX*TPI/1000.
    WBF=250.
    LN=ALOG(FLOAT(N))/ALOG(2.)+.5
    N=2**LN
    DR=DRKM*1000. $ WL=SNORM/FREQ $ FKR=2.*PI/WL
    GW=FGW*WL $ DZ=ZMAX/FLOAT(N)
    ZKM=ZMAX/1000.
    RANGE=NSTEP*DRKM
    WRITE(6,300) FREQ,ZKM ,N,DZ,RANGE,NSTEP,DRKM
   * ,DELC
300 FORMAT(1H1,* ACOUSTIC FREQUENCY  *,F4.0,* HZ*//
   * * OCEAN DEPTH *,F3.1,* KM   NO. OF DEPTH POINTS*,I5,
   * *      STEP SIZE*,F8.2,* M*//
   * * RANGE *,F6.2,* KM   NO. OF RANGE STEPS*,I5,
   * *      STEP SIZE*,F5.2,* KM*//
   * * DELC * ,E12.2,///)
    WRITE(6,100)
    WRITE(6,200)
100 FORMAT(20X,*PLOT OF THE ACOUSTIC FIELD*//
   * 17X,*ALL DIMENSIONS ARE IN KILOMETERS*,//
   * * RANGE / DEPTH ->*/
   * *    ?*/
   * *    ?*)
200 FORMAT(1H0,9X,*0.0*9X*0.5*9X*1.0*9X*1.5*9X*2.0*
   * 9X*2.5*9X*3.0*9X*3.5*9X*4.0*/)
    GO TO 70
    END
```

```
      SUBROUTINE EIGENFN(GAMMA,K,W,WG,DZ,NZ,FZN)
      COMMON /EGNFN/ F(257),G(257),QN(257),QNS(257)
      REAL K,KQ
      DATA C6,C24/.16666666666666,.04166666666666/
      PQ(X)=GAMMAQ*X-KQ
      GAMMAQ=(DZ*GAMMA)**2
      KQ=(DZ*K)**2
      F(1)=F1=FZZ1=0.
      FZ1=DZ
      G(1)=G1=GZ1=GZZ1=0.
      DO 100 I=2,NZ
      F2=F1+.5*FZ1+.125*FZZ1
      G2=G1+.5*GZ1+.125*GZZ1
      PQ2=PQ(QN(I-1))
      F2=F2-C24*(FZZ1+F2*PQ2)
      G2=G2-C24*(GZZ1+G2*PQ2+F2*QN(I-1))
      FZZ2=-F2*PQ2
      GZZ2=-G2*PQ2-F2*QN(I-1)
      F3=F1+FZ1+C6*(FZZ1+2.*FZZ2)
      G3=G1+GZ1+C6*(GZZ1+2.*GZZ2)
      PQ3=PQ(QN(I))
      FZZ3=-F3*PQ3
      GZZ3=-G3*PQ3-F3*QN(I)
      F(I)=F1=F3
      G(I)=G1=G3
      FZ1=FZ1+C6*(FZZ1+4.*FZZ2+FZZ3)
      GZ1=GZ1+C6*(GZZ1+4.*GZZ2+GZZ3)
      FZZ1=FZZ3
  100 GZZ1=GZZ3
      W=-F1
      WG=-G1*DZ**2
      FZN=FZ1
      RETURN
      END
```

```
      SUBROUTINE EIGENVL(GAMMA,K,NORM,ONORM,MODE,MERR,IERR,
     .NZ,DZ,HN,ERR)
      COMMON /EGNFN/ F(257),G(257),QN(257),QNS(257)
      COMMON/IWAVES/END,FINER,A(9)
      REAL K, NORM
      MERR=0
      IERR=0
      DGMAX=.6/HN
      SGN=1.
      IF(MOD(MODE,2).EQ.0) SGN=-1.
      DO 10 I=1,10
      CALL EIGENFN(GAMMA,K,W,WG,DZ,NZ,FZN)
      IF( SGN*WG.LE.0.) GO TO 11
      DGAMMA=W/(2.*GAMMA*WG)
      IF(ABS(DGAMMA).GT.DGMAX) DGAMMA=SIGN(DGMAX,DGAMMA)
      GAMMA=GAMMA-DGAMMA
      IF(ABS(DGAMMA/GAMMA).LE.ERR) GO TO 12
   10 CONTINUE
   11 IERR=1
   12 M=1
      EPS=DZ**2*W/WG
      DO 20 I=1,NZ
   20 F(I)=F(I)-EPS*G(I)
      N1=NZ-1
      DO 25 I=2,N1
      IF((F(I-1)*F(I).LT.0.).OR.F(I).EQ.0.) M=M+1
   25 CONTINUE
      MERR =M-MODE
      IF(MERR.NE.0.OR.IERR.EQ.1) RETURN
      ONORM=-WG*FZN/DZ
      RON=1./SQRT(ONORM)
      SUM=0.
      SUMR=0.
      DO 30 I=1,NZ
      SUM=SUM+F(I)**2
      F(I)=F(I)*(QN(I) + FINER**2)
      SUMR=SUMR + F(I)**2
   30 CONTINUE
      UNORM=1./SQRT(SUMR*DZ)
      DO 31 I=1,NZ
   31 F(I) = F(I)*UNORM
      NORM=DZ*SUM
      RETURN
      END
```

```
      SUBROUTINE FFT842(N2POW,X,Y)
      DIMENSION X(2),Y(2),L(15),CS(2049),SS(2049)
      EQUIVALENCE(L15,L(1)),(L14,L(2)),(L13,L(3)),(L12,L(4)),(L11,L(5)),
     1(L10,L(6)),(L9,L(7)),(L8,L(8)),(L7,L(9)),(L6,L(10)),(L5,L(11)),(L4
     2,L(12)),(L3,L(13)),(L2,L(14)),(L1,L(15))
      DATA LST /0/
      NTHPO =2**N2POW
      N8POW=N2POW/3
      IF(N8POW) 17,3,17
17    LNG=NTHPO
      FLNG=LNG
      IF (LNG-LST) 171,173,171
171   LST=LNG
      DT=6.283185307179/FLNG
      CS(1)=1.
      SS(1)=0.
      TH=0.
      ND=LST/8
      DO 172 I=2,ND
      TH=TH+DT
      CS(I)= COS(TH)
172   SS(I)= SIN(TH)
173   DO 1 IPASS=1,N8POW
      NXTLT =2**(N2POW-3*IPASS)
      LENGT =8*NXTLT
      SC=FLNG/FLOAT(LENGT)
      DO1J=1,NXTLT
      NRG=FLOAT(J-1)*SC+1.5
      C1=CS(NRG)
      S1=SS(NRG)
      C2=C1**2-S1**2
      S2=C1*S1+C1*S1
      C3=C1*C2-S1*S2
      S3=C2*S1+S2*C1
      C4=C2**2-S2**2
      S4=C2*S2+C2*S2
      C5=C2*C3-S2*S3
      S5=C3*S2+S3*C2
      C6=C3**2-S3**2
      S6=C3*S3+C3*S3
      C7=C3*C4-S3*S4
      S7=C4*S3+S4*C3
      DO1ISQLO =LENGT ,NTHPO ,LENGT
      JO=ISQLO -LENGT +J
      J1=JO+NXTLT
      J2=J1+NXTLT
      J3=J2+NXTLT
      J4=J3+NXTLT
      J5=J4+NXTLT
      J6=J5+NXTLT
      J7=J6+NXTLT
      AR0=X(JO)+X(J4)
      AR1=X(J1) + X(J5)
      AR2=X(J2)+X(J6)
      AR3=X(J3)+X(J7)
      AR4=X(JO)-X(J4)
      AR5=X(J1)-X(J5)
```

```
      AR6=X(J2)-X(J6)
      AR7=X(J3)-X(J7)
      AI0=Y(J0)+Y(J4)
      AI1=Y(J1)+Y(J5)
      AI2=Y(J2)+Y(J6)
      AI3=Y(J3)+Y(J7)
      AI4=Y(J0)-Y(J4)
      AI5=Y(J1)-Y(J5)
      AI6=Y(J2)-Y(J6)
      AI7=Y(J3)-Y(J7)
      BR0=AR0+AR2
      BR1=AR1+AR3
      BR2=AR0-AR2
      BR3=AR1-AR3
      BR4=AR4-AI6
      BR5=AR5-AI7
      BR6=AR4+AI6
      BR7=AR5+AI7
      BI0=AI0+AI2
      BI1=AI1+AI3
      BI2=AI0-AI2
      BI3=AI1-AI3
      BI4=AI4+AR6
      BI5=AI5+AR7
      BI6=AI4-AR6
      BI7=AI5-AR7
      X(J0)=BR0+BR1
      Y(J0)=BI0+BI1
      IF(J-1) 2,2,18
18    X(J1)= C4*(BR0-BR1)-S4*(BI0-BI1)
      Y(J1)=C4*(BI0-BI1)+S4*(BR0-BR1)
      X(J2)=C2*(BR2-BI3)-S2*(BI2+BR3)
      Y(J2)=C2*(BI2+BR3)+S2*(BR2-BI3)
      X(J3)=C6*(BR2+BI3)-S6*(BI2-BR3)
      Y(J3)=C6*(BI2-BR3)+S6*(BR2+BI3)
      TR= 0.7071067812*(BR5-BI5)
      TI=0.7071067812*(BR5+BI5)
      X(J4)=C1*(BR4+TR)-S1*(BI4+TI)
      Y(J4)=C1*(BI4+TI)+S1*(BR4+TR)
      X(J5)=C5*(BR4-TR)-S5*(BI4-TI)
      Y(J5)=C5*(BI4-TI)+S5*(BR4-TR)
      TR=-0.7071067812*(BR7+BI7)
      TI=0.7071067812*(BR7-BI7)
      X(J6)=C3*(BR6+TR)-S3*(BI6+TI)
      Y(J6)=C3*(BI6+TI)+S3*(BR6+TR)
      X(J7)=C7*(BR6-TR)-S7*(BI6-TI)
      Y(J7)=C7*(BI6-TI)+S7*(BR6-TR)
      GO TO 1
2     X(J1)=BR0-BR1
      Y(J1)=BI0-BI1
      X(J2)=BR2-BI3
      Y(J2)=BI2+BR3
      X(J3)=BR2+BI3
      Y(J3)=BI2-BR3
      TR=0.7071067812*(BR5-BI5)
      TI=0.7071067812*(BR5+BI5)
      X(J4)=BR4+TR
```

```
      Y(J4)=BI4+TI
      X(J5)=BR4-TR
      Y(J5)=BI4-TI
      TR=-0.7071067812*(BR7+BI7)
      TI=0.7071067812*(BR7-BI7)
      X(J6)=BR6+TR
      Y(J6)=BI6+TI
      X(J7)=BR6-TR
      Y(J7)=BI6-TI
 1    CONTINUE
 3    IF(N2POW-3*N8POW-1)5,6,7
 6    DO61J=1,NTHPO ,2
      R1=X(J)+X(J+1)
      X(J+1)=X(J)-X(J+1)
      X(J)=R1
      FI1=Y(J)+Y(J+1)
      Y(J+1)=Y(J)-Y(J+1)
 61   Y(J)=FI1
      GOTO5
7     DO71J1=1,NTHPO ,4
      J2=J1+1
      J3=J2+1
      J4=J3+1
      R1=X(J1)+X(J3)
      R2=X(J1)-X(J3)
      R3=X(J2)+X(J4)
      R4=X(J2)-X(J4)
      FI1=Y(J1)+Y(J3)
      FI2=Y(J1)-Y(J3)
      FI3=Y(J2)+Y(J4)
      FI4=Y(J2)-Y(J4)
      X(J1)=R1+R3
      Y(J1)=FI1+FI3
      X(J2)=R1-R3
      Y(J2)=FI1-FI3
      X(J3)=R2-FI4
      Y(J3)=FI2+R4
      X(J4)=R2+FI4
 71   Y(J4)=FI2-R4
 5    DO51J=1,15
      L(J)=1
      IF(J-N2POW) 19,19,51
19    L(J) = 2**(N2POW+1-J)
 51   CONTINUE
      IJ=1
      DO8J1=1,L1
      DO8J2=J1,L2,L1
      DO8J3=J2,L3,L2
      DO8J4=J3,L4,L3
      DO8J5=J4,L5,L4
      DO8J6=J5,L6,L5
      DO8J7=J6,L7,L6
      DO8J8=J7,L8,L7
      DO8J9=J8,L9,L8
      DO8J10=J9,L10,L9
      DO8J11=J10,L11,L10
      DO8J12=J11,L12,L11
```

```
      DO8J13=J12,L13,L12
      DO8J14=J13,L14,L13
      DO8JI=J14,L15,L14
      IF(IJ-JI) 20,8,8
20    R=X(IJ)
      X(IJ)=X(JI)
      X(JI)=R
      FI=Y(IJ)
      Y(IJ)=Y(JI)
      Y(JI)=FI
8     IJ=IJ+1
      RETURN
      END
```

```
      SUBROUTINE INIT
      COMMON /ACOUST/ UR(2048),UI(2048)
      COMMON /NFACTS/ N,LN,NR,NTLOSS,NIT
      COMMON /AFACTS/ FREQ,SNORM,ZMAX,GW,FGW,DR,FKR,DZ,WL,PI,GD
      PROF(X)=SGAIN*EXP(-((X-GD)/GW)**2)
      SGAIN=(.9144/GW)*SQRT(WL/PI)
      DO 10 J=1,N
      DEPTH=DZ*FLOAT(J)
      UR(J)=PROF(DEPTH)-PROF(-DEPTH)
10    UI(J)=0.
      RETURN
      END
```

```
      SUBROUTINE PHASE1
      COMMON /PHASES/ SK(1024),CK(1024),SM(1024),CM(1024)
      COMMON /NFACTS/ N,LN,NR,NTLOSS,NIT
      COMMON /AFACTS/ FREQ,SNORM,ZMAX,GW,FGW,DR,FKR,DZ,WL,PI,GD
      FK=PI/ZMAX
      FN=FLOAT(N*2)
      DO 10 K=1,N
      AK=FLOAT(K)*FK/FKR
      ANG=.5*DR*FKR*AK**2
      SK(K)=SIN(ANG)/FN
10    CK(K)=COS(ANG)/FN
      RETURN
      END
```

```
      SUBROUTINE PHASE2
      REAL SSM(1024),SSF(1024),ALOSS(1024)
      COMMON /PHASES/ SK(1024),CK(1024),SM(1024),CM(1024)
      COMMON /NFACTS/ N,LN,NR,NTLOSS,NIT
      COMMON /AFACTS/ FREQ,SNORM,ZMAX,GW,FGW,DR,FKR,DZ,WL,PI,GD
      COMMON /MUNK/ CA,ZA,ZW,GEE
      DATA ISTRT /0/
      IF(ISTRT .GT. 0) GOTO 100
      ISTRT=1
      DLW=.04*ZMAX
      DLP=.05
      DO 10 J=1,N
      DEPTH=DZ*FLOAT(J)
      BLOSS=DLP*EXP(-((DEPTH-ZMAX)/DLW)**2)
   10 ALOSS(J)=EXP(-DR*BLOSS)
      DO 20 J=1,N
      DEPTH=DZ*FLOAT(J)
      ARG=2.*(DEPTH-ZA)/ZW
   20 SSM(J)=CA+GEE*(ZW/2.)*(ARG-1.+EXP(-ARG))
      DO 30 J=1,N
      EN=SNORM/SSM(J)
   30 SSM(J)=.5*FKR*DR*(EN+1.)*(EN-1.)
  100 CONTINUE
      CALL RNDMF(SSF)
      DO 120 J=1,N
      ANG=SSM(J)+SSF(J)
      SM(J)=ALOSS(J)*SIN(ANG)
  120 CM(J)=ALOSS(J)*COS(ANG)
      RETURN
      END
```

```
      SUBROUTINE PRINTP
      COMMON/ACOUST/UR(2048),UI(2048)
      COMMON/NFACTS/N,LN,NR,NTLOSS,NIT
      COMMON/VAR/R,IR
      INTEGER P(32)
      ISK=N/32
      RAN=R/1000.
      DO 10 J=1,32
      I=(J-1)*ISK+1
      POW=UR(I)**2+UI(I)**2
   10 P(J)=-10.*ALOG10(POW/R+1.E-100)
      WRITE(6,20) RAN,P,IR
   20 FORMAT(F7.2,3X,32I3,I5)
      RETURN $ END
```

```
      FUNCTION PS(K,MODE)
      REAL K
      COMMON /IWAVES/ ENO,FINER,BZ,EZMAX,NZ,AKMAX,NK,NMODE,
     1 SIG,TIW,JSTAR
      DATA ISTRT /0/
      DATA PI /3.1415926536/
      H(X)=(TIW-1.)*(1.+X)**(-TIW)
      IF(ISTRT.NE.0) GO TO 100
      ISTRT=1
      S=FINER/ENO
      AKO=1./BZ
      AA=FLOAT(JSTAR)*PI*S*AKO
      AK1=AKMAX/FLOAT(NK)
      COEF=AK1*SIG**2*(BZ/3.)*(4.*S)*AKO
100   ALAM=FLOAT(MODE)/FLOAT(JSTAR)
      AKREF=AA*ALAM
      PS=COEF*K**2*ALAM*H(ALAM)/(K**2+AKREF**2)**2
      RETURN
      END
```

```
      SUBROUTINE RNDMF(SSF)
      REAL SSF(1),SST(257),YZ(257),AZ(257)
      COMMON /IWAVES/ ENO,FINER,BZ,EZMAX,NZ,AKMAX,NK,NMODE,
     1 SIG,TIW,JSTAR
      LARGE EFR(256,257),EFI(256,257)
      COMMON /NFACTS/ N,LN,NR,NTLOSS,NIT
      COMMON /AFACTS/ FREQ,SNORM,ZMAX,GW,FGW,DR,FKR,DZ,WL,PI
      COMMON /VAR/ R,IR,T,IT
      REAL ESR(256),ESI(256)
      REAL SP(4)
      DATA ITT /0/
      IF(IT.EQ.ITT) GOTO 100
      ITT=IT
      DO 1 I=1,N
    1 SSF(I)=0.
      IF(SIG.EQ.0.) GOTO 100
      NX=2*NK
      TPI=2.*PI
      DX=PI/AKMAX
      SR2=1./SQRT(2.)
      FCTR=FKR*DR
      DEZ=EZMAX/FLOAT(NZ-1)
      RDEZS=1./DEZ**2
      CALL ZMODEJ
      LNX=ALOG(FLOAT(NX))/ALOG(2.)+.5
      DO 2 IZ=1,NZ
      DO 21 IL=1,NX
      ESR(IL)=EFR(IL,IZ)
   21 ESI(IL)=EFI(IL,IZ)
      CALL FFT842(LNX,ESR,ESI)
      DO 22 IL=1,NX
      EFR(IL,IZ)=ESR(IL)
   22 EFI(IL,IZ)=ESI(IL)
    2 CONTINUE
      DSUM=0.
      L=0
      DO 5 IZ=1,NZ
      SUM=0.
      DO 4 IX=1,NX
      EFR(IX,IZ)=SR2*(EFR(IX,IZ)+EFI(IX,IZ))
    4 SUM=SUM+EFR(IX,IZ)**2
      SUM=SUM/FLOAT(NX)
      L=L+1
      SP(L)=SUM
      IF(L.LT.4) GOTO 5
      L=0
    5 DSUM=DSUM+SUM
      DSUM=DEZ*DSUM
      WRITE(6,91) DSUM
   90 FORMAT(1H ,I5,4X,4E14.5)
   91 FORMAT(1H0,* Z INTEGRAL OF DG/G SQUARED = *,E14.5,/)
      IRSKP=INT(DX/DR+.1)
      IZSKP=FLOAT(N)/FLOAT(NZ-1)+.5
      RRSKP=1./FLOAT(IRSKP)
      RZSKP=1./FLOAT(IZSKP)
      AZ(1)=AZ(NZ)=YZ(1)=0.
      NZ1=NZ-1
```

```
  100  CONTINUE
       IF(SIG.EQ.0) RETURN
       IX=MOD((IR-1)/IRSKP,NX)+1
       IXP1=IX+1 $ IF(IX.EQ.NX)IXP1=1
       IF(IRSKP.GT.1) GOTO 108
       DO 104 IZ=1,NZ
  104  SST(IZ)=EFR(IX,IZ)
       GO TO 115
  108  JR=MOD(IR-1,IRSKP)
       U=FLOAT(JR)*RRSKP
       V=1.-U
       DO 110 IZ=1,NZ
  110  SST(IZ)=U*EFR(IXP1,IZ)+V*EFR(IX,IZ)
  115  CONTINUE
       DO 120 IZ=2,NZ1
       YZ(IZ)=1./(4.-YZ(IZ-1))
       TEMP=(SST(IZ+1)-2.*SST(IZ)+SST(IZ-1))*RDELS
  120  AZ(IZ)=(TEMP-AZ(IZ-1))*YZ(IZ)
       DO 130 IB=2,NZ1
       IZ=NZ+1-IB
  130  AZ(IZ)=AZ(IZ)-YZ(IZ)*AZ(IZ+1)
       DO 140 I=1,NZ1
       DO 140 J=1,IZSKP
       IZ=IZSKP*(I-1)+J
       U=FLOAT(J)*RZSKP
       V=1.-U
       SSF(IZ)=U*SST(I+1)+V*SST(I)-
      1 DZ**2*U*V*(AZ(I)*(1.+V)+AZ(I+1)*(1.+U))
  140  CONTINUE
       DO 150 I=1,N
  150  SSF(I)=-FCTR*SSF(I)
       RETURN
       END
```

```
      SUBROUTINE TAPEIW(IFL)
      COMMON/AFACTS/AF(11)
      COMMON/NFACTS/BNF(5)
      COMMON/MUNK/UM(4)
      COMMON/IWAVES/BIW(11)
      COMMON/STEP/STE(4)
      COMMON/SAV/SAVR(100,4),SAVI(100,4)
      COMMON/ACOUST/UR(2048),UI(2048)
      COMMON/VAR/R,IR,T,IT
      EQUIVALENCE (NSAV,STE(3))
      DIMENSION B(2850)
      GO TO (100,200,300) IFL
  100 CONTINUE
      L=0
      DO 1 I=1,11
      L=L+1
    1 B(L)=AF(I)
      DO 2 I=1,5
      L=L+1
    2 B(L)=BNF(I)
      DO 3 I=1,4
      L=L+1
    3 B(L)=UM(I)
      DO 4 I=1,11
      L=L+1
    4 B(L)=BIW(I)
      DO 5 I=1,4
      L=L+1
    5 B(L)=STE(I)
      WRITE(10) L,(B(I),I=1,L)
      RETURN
  200 CONTINUE
      B(1)=R
      B(2)=T
      L=2
      DO 31 I=1,1024
      L=L+1
   31 B(L)=UR(I)
      DO 32 I=1,1024
      L=L+1
   32 B(L)=UI(I)
      DO 33 I=1,4
      DO 33 J=1,NSAV
      L=L+1
      B(L)=SAVR(J,I)
      L=L+1
   33 B(L)=SAVI(J,I)
      WRITE(10) L,(B(I),I=1,L)
      RETURN
  300 CONTINUE
      ENDFILE 10
      ENDFILE 10
      RETURN
      END
```

```
      SUBROUTINE UWS
      COMMON /ACOUST/ UR(2048),UI(2048)
      COMMON /PHASES/ SK(1024),CK(1024),SM(1024),CM(1024)
      COMMON /NFACTS/ N,LN,NR,NTLOSS,NIT
      COMMON /AFACTS/ FREQ,SNORM,ZMAX,GW,FGW,DR,FKR,DZ,WL,PI,GO
      NM1=N-1
      N2=N*2
      DO 10 J=1,NM1
      UR(J+N)=-UR(N-J)
   10 UI(J+N)=-UI(N-J)
      UR(N2)=0.
      UI(N2)=0.
      CALL FFT842(LN+1,UR,UI)
      DO 20 J=1,NM1
      JP1=J+1
      TEMP=CK(J)*UR(JP1)-SK(J)*UI(JP1)
      UI(JP1)=-CK(J)*UI(JP1)-SK(J)*UR(JP1)
      UR(JP1)=TEMP
      JN2=N2+1-J
      TEMP=CK(J)*UR(JN2)-SK(J)*UI(JN2)
      UI(JN2)=-CK(J)*UI(JN2)-SK(J)*UR(JN2)
   20 UR(JN2)=TEMP
      UR(1)=UI(1)=0.
      UR(N+1)=UI(N+1)=0.
      CALL FFT842(LN+1,UR,UI)
      DO 30 J=1,N
      TEMP=CM(J)*UR(J)-SM(J)*UI(J)
      UI(J)=-CM(J)*UI(J)-SM(J)*UR(J)
   30 UR(J)=TEMP
      RETURN
      END
```

```
      SUBROUTINE ZMODEJ
      COMMON /IWAVES/ ENO,FINER,BZ,EZMAX,NZ,AKMAX,NK,NMODE,
     1 SIG,TIW,JSTAR
      LARGE EFR(256,257),EFI(256,257)
      COMMON /EGNFN/ F(257),G(257),QN(257),QNS(257)
      COMMON /VAR/ R,IR,T,IT
      REAL TK(257),AR(256,24),AI(256,24)
      REAL GSV(256,24)
      REAL K,KMAX,NORM,KCY
      DATA PI,ERR /3.1415926536,1.E-10/
      DATA ISTRT /0/
      IF(ISTRT.NE.0) GOTO 20
      ISTRT=1
      TPI=2.*PI
      KMAX=AKMAX $ ZMAX=EZMAX
      DZ=ZMAX/(NZ-1) $ DK=AKMAX/FLOAT(NK)
      NK2=NK*2
      DUM=0
      DO 10 I=1,NZ
      Z=DZ*(I-1)
      TEMP=ENO**2*EXP(-2.*Z/BZ)-FINER**2
      TEMP=AMAX1(0.,TEMP)
      QN(NZ+1-I)=TEMP
   10 QNS(NZ+1-I)=SQRT(TEMP)
      HN=ENO*BZ*(1.-EXP(-ZMAX/BZ))
      DO 12 IK=1,NK
   12 TK(IK)=DK*(IK-1)
   20 CONTINUE
      IF(IT.NE.1) GO TO 26
      DO 25 MODE=1,NMODE
      DO 24 IK=1,NK2
      K=DK*AMINO(IK-1,NK2+1-IK)
      POW=-2.*PS(K,MODE)*ALOG(RANF(DUM)+1.E-100)
      AMP=SQRT(POW)
      ANG=TPI*RANF(DUM)
      AR(IK,MODE)=AMP*COS(ANG)
   24 AI(IK,MODE)=AMP*SIN(ANG)
      AR(NK+1,MODE)=0.
   25 AI(NK+1,MODE)=0.
   26 CONTINUE
      DO 27 IZ=1,NZ
      DO 27 IK=1,NK2
      EFR(IK,IZ)=0.
27    EFI(IK,IZ)=0.
      DO 30 MODE=1,NMODE
      GAMMA=(FLOAT(MODE)-.25)*PI/HN
      DG=DDG=0.
      DO 30 IK=1,NK
      K=TK(IK)
      GAMMA=GAMMA+DK*(DG+.5*DDG)
      IF(IT.NE.1) GAMMA=GSV(IK,MODE)
      DG1=DG
      CALL EIGENVL(GAMMA,K,NORM,ONORM,MODE,MERR,IERR,
     .NZ,DZ,HN,ERR)
      IF(MERR.EQ.0.AND.IERR.EQ.0) GO TO 33
      KCY=500.*K/PI
      PRINT 302,MODE,KCY,MERR,IERR
```

```
302 FORMAT(//40X,29HEIGENVL FAILED TO CONVERGE AT,/
   * 45X,5HMODE ,I2,/45X,11HWAVENUMBER ,F 8.2/
   * 45X,7HMERR = ,I2/45X,7HIERR = ,I2)
    STOP
33  RAT=NORM/UNORM
    DG=K*RAT/GAMMA
    DDG=DG-DG1
    IF(IK.EQ.1) DDG=DK*RAT/GAMMA
    IF(IT.EQ.1) GSV(IK,MODE)=GAMMA
    FIW=SQRT(FINER**2+(K/GAMMA)**2)
    CW=COS(FIW*T)
    SW=SIN(FIW*T)
    IL=NK2+2-IK
    IF(IK.EQ.1) IL=NK+1
    AR1=AR(IK,MODE)
    AI1=AI(IK,MODE)
    AR2=AR(IL,MODE)
    AI2=AI(IL,MODE)
    DO 35 IZ=1,NZ
    JZ=NZ+1-IZ
    EFR(IK,IZ)=EFR(IK,IZ)+F(JZ)*(AR1*CW-AI1*SW)
    EFI(IK,IZ)=EFI(IK,IZ)+F(JZ)*(AR1*SW+AI1*CW)
    EFR(IL,IZ)=EFR(IL,IZ)+F(JZ)*(AR2*CW-AI2*SW)
 35 EFI(IL,IZ)=EFI(IL,IZ)+F(JZ)*(AR2*SW+AI2*CW)
30  CONTINUE
    RETURN
    END
```

LOAD MAP.

FL REQUIRED TO LOAD 147500
FL REQUIRED TO RUN 137000
INITIAL TRANSFER TO USER - 27611

BLOCK ASSIGNMENTS.

BLOCK	ADDRESS	LENGTH	FILE
/NFACTS/	100	5	
/AFACTS/	105	13	
/VAR/	120	4	
/ACOUST/	124	10000	
/STOP/	10124	1	
/PHASES/	10125	10000	
/BFOR/	20125	6000	
/MUNK/	26125	4	
/IWAVES/	26131	13	
/SAV/	26144	1440	
/STEP/	27604	4	
USER	27610	1541	LGO
PRINTP	31351	137	LGO
TAPEIW	31510	5660	LGO
DAYFOOL	37370	170	LGO
RNDMF	37560	3135	LGO
/EGNFN/	42715	2004	
ZMODEJ	44721	45154	LGO
EIGENVL	112075	230	LGO
EIGENFN	112325	236	LGO
PS	112563	131	LGO
UWS	112714	134	LGO
INIT	113050	75	LGO
PHASE1	113145	54	LGO
PHASE2	113221	6161	LGO
FFT642	121402	11242	LGO
ACGOER	132644	10	SYSLIB
ALNLOG	132654	110	SYSLIB
ENDFIL	132764	11	SYSLIB
EXP	132775	53	SYSLIB
IBATEX	133050	31	SYSLIB
OUTPTB	133101	31	SYSLIB
OUTPTC	133132	50	SYSLIB
RANF	133202	24	SYSLIB
RBAREX	133226	57	SYSLIB
RUNSYS	133305	303	SYSLIB
SINCOS	133610	72	SYSLIB
SQRT	133702	42	SYSLIB
STATUS	133744	26	SYSLIB
TIMES	133772	37	SYSLIB
CPUCIO	134031	506	SYSLIB
CPUSYS	134537	53	SYSLIB
KODER	134612	1235	SYSLIB
RUNIOP	136047	323	SYSLIB
SYSTM	136372	322	SYSLIB
//	136714	36	

Appendix

CUBIC SPLINE INTERPOLATION

Appendix

CUBIC SPLINE INTERPOLATION

The subroutine RNDMF uses cubic splines to interpolate the velocity profiles from the coarse mesh on which the random internal wave field is computed, to the finer mesh on which the acoustic field is stored. The theory behind this is as follows.

We want an interpolation formula for the function v(z), given the mesh points z_i (i = 1,2...,n+1) and function values v_i (i=1,2,...,n+1). Let

$$\Delta z_i = z_{i+1} - z_i \quad , \quad i = 1,2,\ldots,n \tag{A-1a}$$

$$\Delta v_i = (v_{i+1} - v_i)/\Delta z_i \quad , \quad i = 1,2,\ldots,n \quad . \tag{A-1b}$$

In the interval $z_i \le z \le z_{i+1}$, define the weight functions

$$w = (z - z_i)/\Delta z_i \tag{A-2a}$$

$$\bar{w} = 1 - w \quad . \tag{A-2b}$$

In each such interval, write v(z) as a cubic polynomial continuous at the mesh points as follows:

$$\begin{aligned} v(z) &= \bar{w}v_i + wv_{i+1} + (\Delta z_i)^2 \left[a_i(\bar{w}^3 - \bar{w}) + a_{i+1}(w^3 - w)\right] \\ &= \bar{w}v_i + wv_{i+1} - (\Delta z_i)^2 w\bar{w}\left[a_i(\bar{w}+1) + a_{i+1}(w+1)\right] \quad . \end{aligned} \tag{A-3}$$

The first two terms give a linear interpolation and the last terms give a second-order correction (cubic in z) using the undetermined coefficients a_i which are essentially the second derivatives at the mesh points. From Eq. (A-3), we find

$$v'(z) = \Delta v_i + \Delta z_i \left| -a_i \left(3\bar{w}^2 - 1\right) + a_{i+1}\left(3w^2 - 1\right) \right| \quad , \qquad \text{(A-4)}$$

$$v''(z) = 6\left| a_i \bar{w} + a_{i+1} w \right| \quad . \qquad \text{(A-5)}$$

Equations (A-3) and (A-5) show that the selected way of writing v(z) makes both v and v'' continuous functions of z [and incidentally Eq. (A-5) shows that $v''(z_i) = 6a_i$]. In order to make $v'(z)$ continuous, we match values of $v'(z_{i+1})$ using Eq. (A-4) in the two neighboring intervals. This yields the conditions

$$\Delta v_i + \Delta z_i \left(a_i + 2a_{i+1}\right) = \Delta v_{i+1} - \Delta z_{i+1}\left(2a_{i+1} + a_{i+2}\right)$$

which can be put in the form:

$$\Delta z_i a_i + 2\left(\Delta z_i + \Delta z_{i+1}\right) a_{i+1} + \Delta z_{i+1} a_{i+2} = \Delta v_{i+1} - \Delta v_i \qquad \text{(A-6)}$$

for $i = 1,2,\ldots,n-1$.

To make this system of linear equations for the a_i determinate, we choose $a_1 = a_{n+1} = 0$. This amounts to the assumption that v(z) is linear in z at the two end points of the interpolation region (top and bottom of the ocean).

Equation (A-6) is a tri-diagonal system and is most efficiently solved numerically using the "double sweep" method. Look for a solution of the form

$$a_i = r_{i+1} - s_{i+1} a_{i+1} \quad , \; i = 1,\ldots,n \quad . \qquad \text{(A-7)}$$

Substituting Eq. (A-7) into (A-8) gives recursion relations for r_i and s_i as follows:

$$a_i = \frac{1}{p_i}\left[\left(\Delta v_i - \Delta v_{i-1}\right) - \Delta z_{i-1} r_i\right] - \frac{\Delta z_i}{p_i} a_{i+1} \qquad \text{(A-8)}$$

where $p_i = 2(\Delta v_{i-1} + \Delta v_i) - \Delta z_{i-1} s_i$, $i = 2,\ldots,n$.

Combining Eqs. (A-7) and (A-8) we obtain

$$s_{i+1} = \frac{\Delta z_i}{p_i} \quad , \quad i = 2,\ldots,n \quad , \qquad \text{(A-9)}$$

$$r_{i+1} = \left[\Delta v_i - \Delta v_{i-1} - \Delta z_{i-1} r_i\right] / p_i \quad , \; i = 2,\ldots,n \quad . \qquad \text{(A-10)}$$

The starting values of these right-sweeping recursion relations are $r_2 = s_2 = 0$ (as follows from $a_1 = 0$). The full procedure is therefore the following. Starting with $r_2 = s_2 = 0$, compute p_2 from Eq. (A-8), then compute s_3 and r_3 from Eqs. (A-9) and (A-10), and again use Eq. (A-8) to compute p_3, then Eqs. (A-9) and (A-10) to compute s_4 and r_4, and so on until one obtains s_{n+1} and r_{n+1}; then use the left-sweeping recursion relation in Eq. (A-7) starting with $a_{n+1} = 0$ to compute successively a_n, $a_{n-1},\ldots,a_3$, a_2 .

The values of a_i computed in this way are then used in Eq. (A-3) to compute interpolated values of v(z) where needed.

A special case of this method is when Δz_i = const (say, $\Delta z_i = \Delta z$) for all i . Equations (A-8), (A-9), and (A-10) can then be simplified to:

$$s_{i+1} = \frac{1}{4 - s_i} \quad , \qquad \text{(A-11)}$$

$$r_{i+1} = \left| \left(\Delta v_i - \Delta v_{i-1} \right) / (\Delta z)^2 - r_i \right| \; s_{i+1} \quad , \qquad \text{(A-12)}$$

for $i = 2,\ldots,n$. Equation (A-7) is then used to compute a_i , $i = n,\ldots,2$; and Eq. (A-3) gives $v(z)$ for any z.

REFERENCES

1. M. Leontovich and V. Fok, "Solution of the Problem of Propagation of Electromagnetic Waves Along the Earth's Surface by the Parabolic Equation Method," Zh. Eksp. Teor. Fiz., Vol. 16, p. 557 (1946).

2. F. D. Tappert and R. H. Hardin, in "A Synopsis of the AESD Workshop on Acoustic Modeling by Non Ray Techniques, 22-25 May 1973, Washington, D.C.," AESD TN-73-05, Office of Naval Research, Arlington, VA. (November 1973).

3. F. D. Tappert, "Parabolic Equation Method in Underwater Acoustics," J. Acoust. Soc. Am., Vol. 55, S34 (1974).

4. C. Garrett and W. Munk, Geophysical Fluid Dynamics, Vol. 2, pp. 225-264 (1972); C. Garrett and W. H. Munk, J. Geophysical Res. Vol. 80, 291 (1974); and W. H. Munk, private communication (1974).

5. W. Munk, J. Acoust. Soc. Am., Vol. 55, pp. 220-226 (1974).

6. S. M. Flatté and F. D. Tappert, "Calculation of the Effect of Internal Waves on Oceanic Sound Transmission," accepted for publication in the J. Acoust. Soc. Am.

7. M. Milder, "Users Manual for the Computer Program ZMODE," RDA-TR-2701-001, R&D Associates, Santa Monica, Calif. (July 1973).

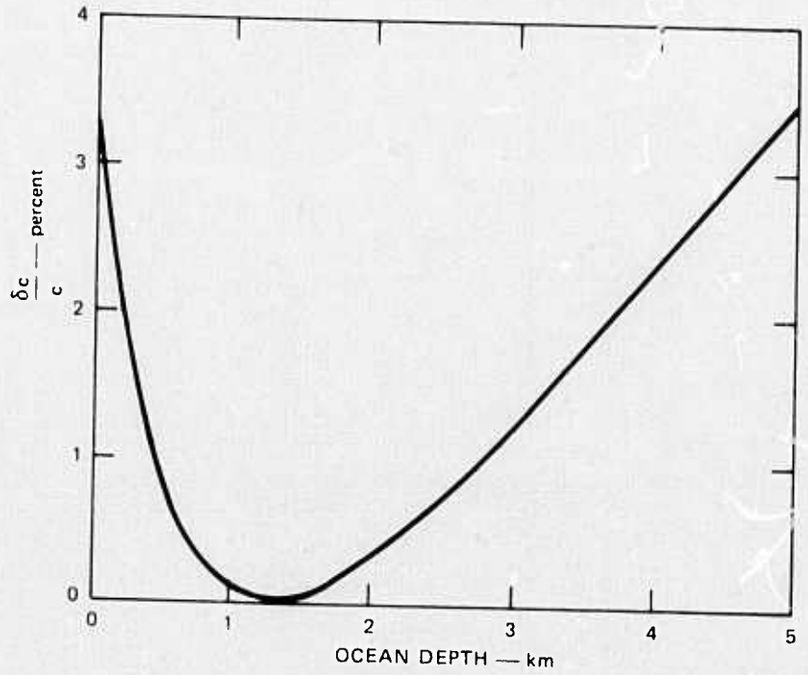

FIGURE 1 DETERMINISTIC SOUND-SPEED PROFILE AS A FUNCTION OF OCEAN DEPTH. The value of c at the minimum (z_A = 1300 m) is $c(z_A)$ = 1500 m/s.

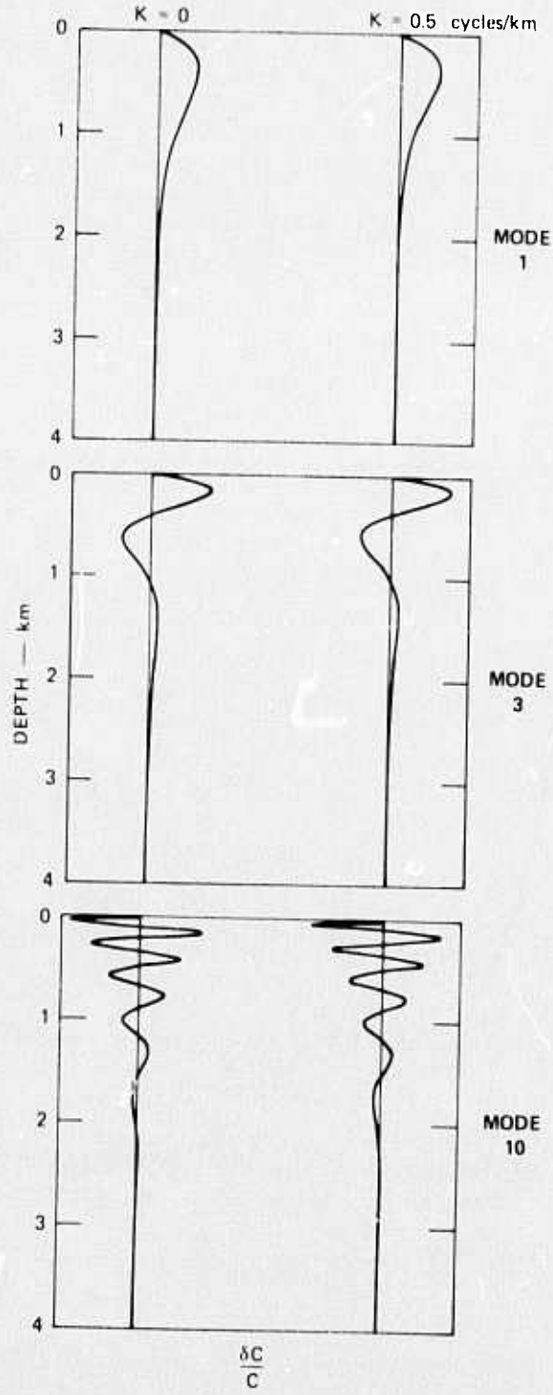

FIGURE 2 SOUND-SPEED PROFILES DUE TO INTERNAL-WAVE MODES. Realistic internal-wave spectra have significant intensities for horizontal wave number, k, less than about 0.5 cycles/km. Note that the major internal-wave contributions to sound-speed fluctuations occur at depths less than 1 km.

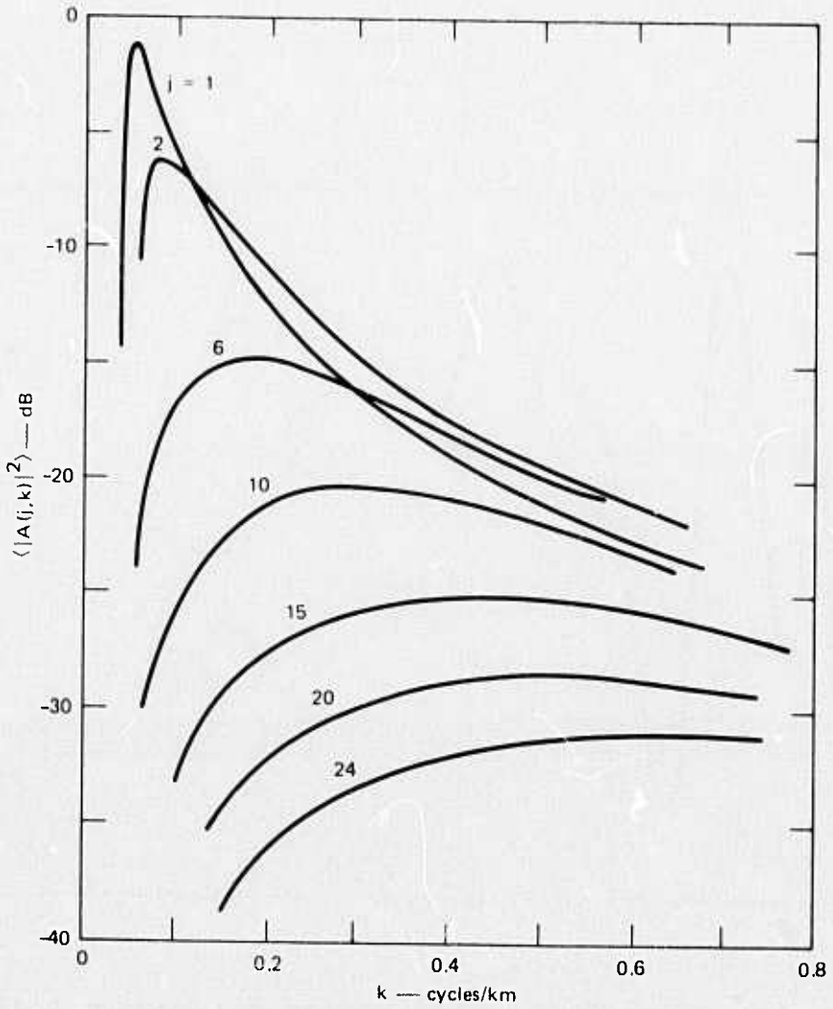

FIGURE 3 INTERNAL-WAVE SPECTRUM AS A FUNCTION OF MODE NUMBER j AND HORIZONTAL WAVE-NUMBER k. Although large mode numbers contribute verry little to the overall spectrum, they are crucial to understanding acoustic effects, since their vertical structure allows them to act as a scatterer of acoustic energy more readily than the relatively structureless low modes.

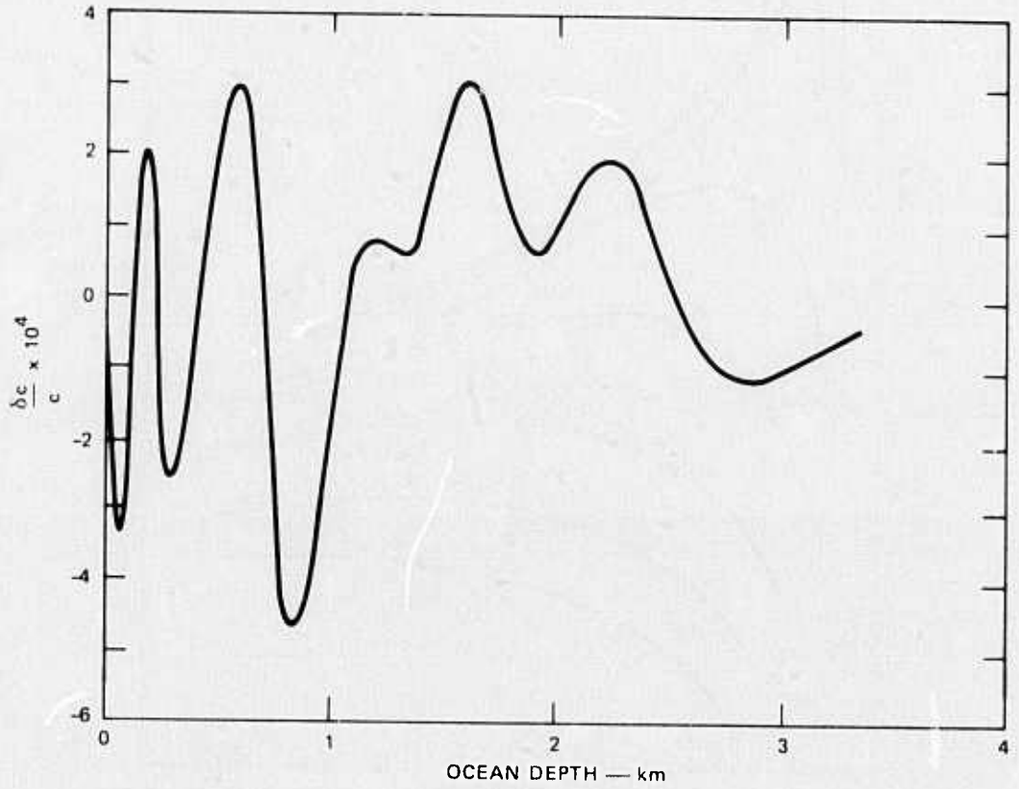

FIGURE 4 TYPICAL SOUND-SPEED FLUCTUATION PROFILE INDUCED BY INTERNAL WAVES

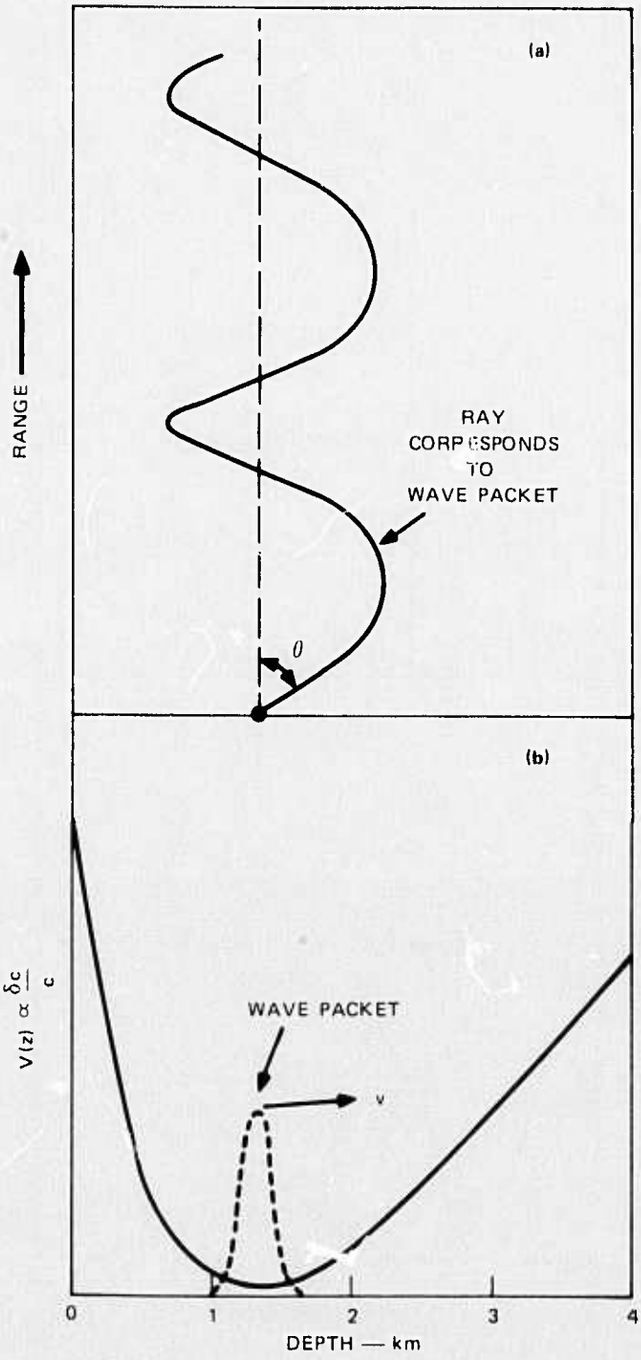

FIGURE 5 ANALOGY BETWEEN (a) AN ACOUSTIC RAY PROPAGATING IN A SOUND CHANNEL CHARACTERIZED BY c(z), AND (b) A SCHRÖDINGER-EQUATION WAVE PACKET IN A POTENTIAL WELL V(z)

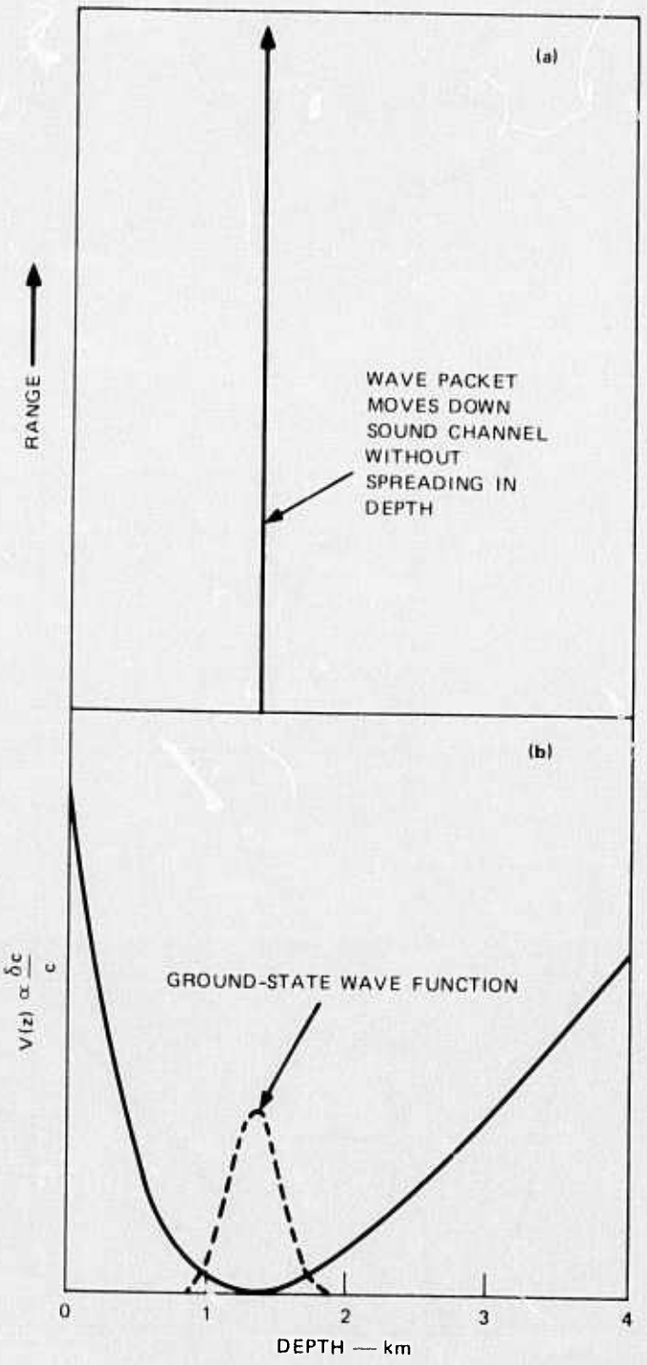

FIGURE 6 ANALOGY BETWEEN (a) AN ACOUSTIC-WAVE FUNCTION TRAVELING DOWN THE SOUND CHANNEL WITHOUT SPREADING IN DEPTH, AND (b) A SCHRÖDINGER-EQUATION GROUND-STATE WAVE FUNCTION IN A POTENTIAL WELL $V(z)$. Time in the Schrödinger situation corresponds to range in the acoustic case.

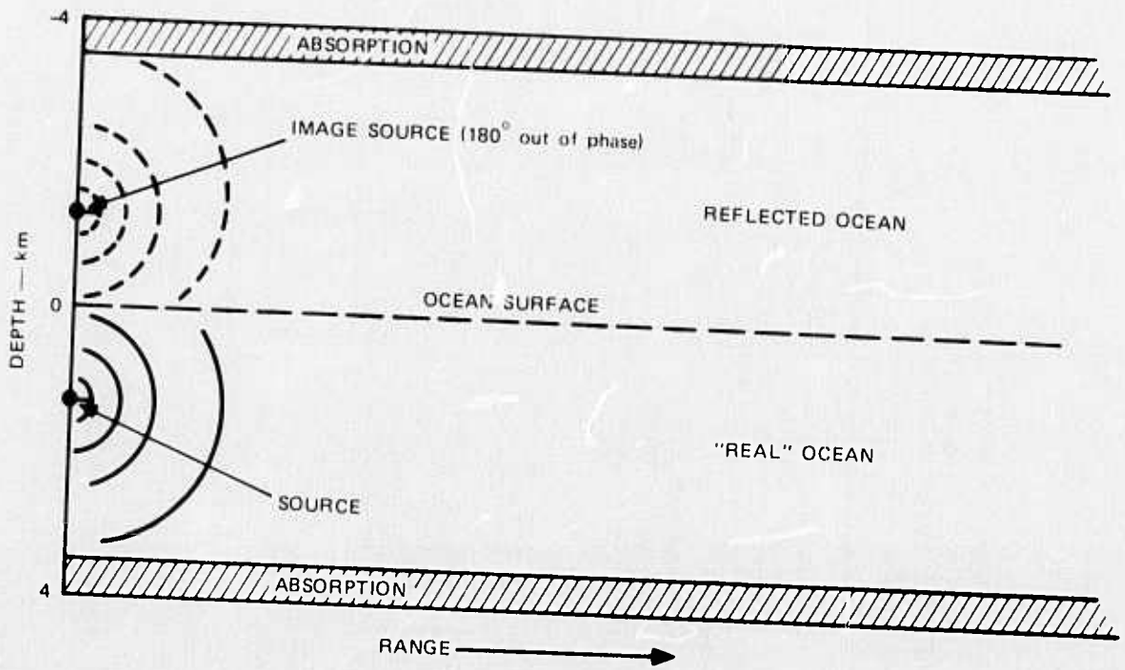

FIGURE 7 DIAGRAM OF BOUNDARY CONDITIONS AND SOURCE GEOMETRY IN OUR NUMERICAL SIMULATION. The image source in the reflected ocean automatically creates the proper ocean surface boundary condition (a perfect reflector). The absorption at the ocean bottom is a smooth function of depth, so that as little energy as possible is reflected.

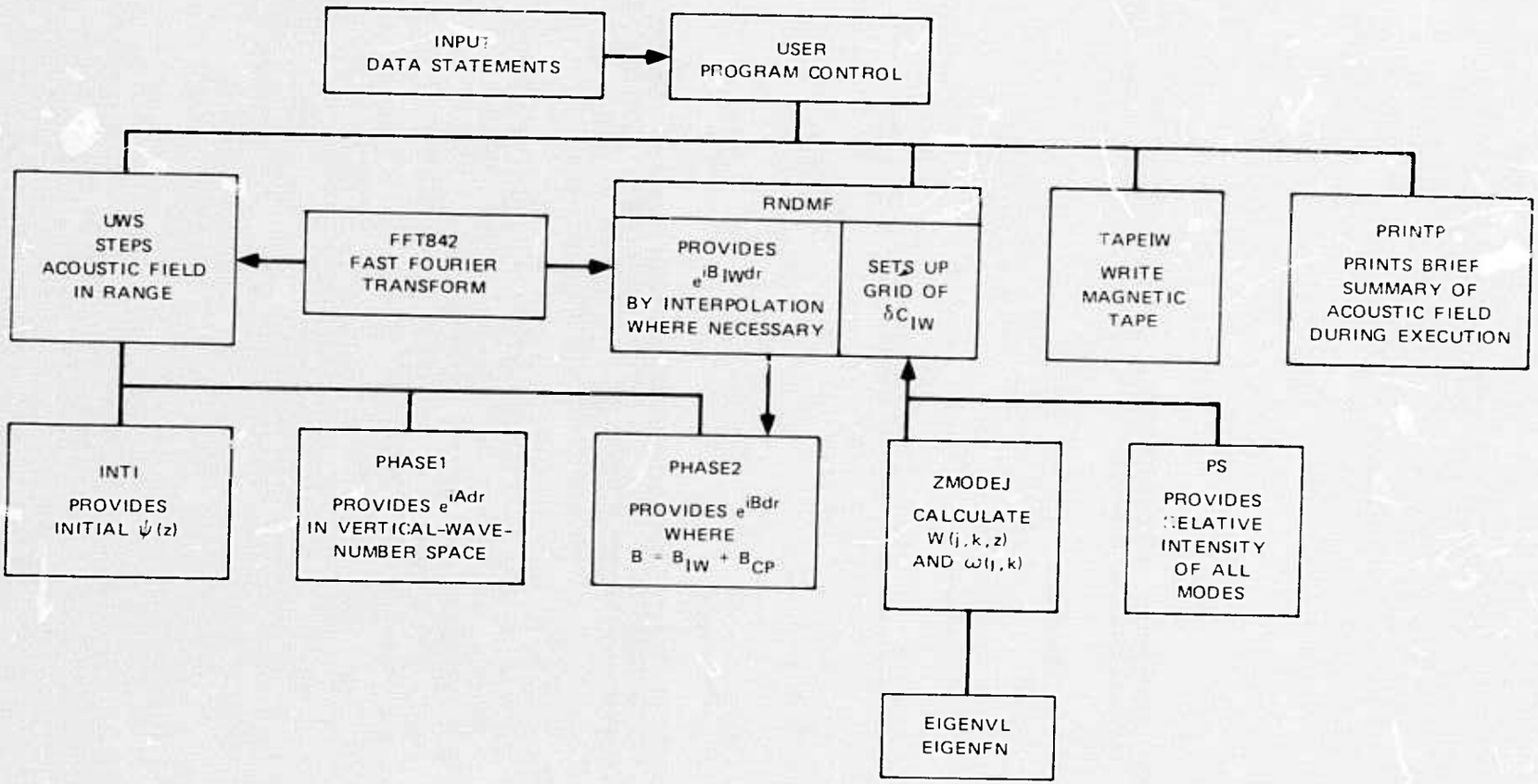

FIGURE 8 CODE ORGANIZATION

DISTRIBUTION LIST

DISTRIBUTION LIST

Dr. Henry D. I. Abarbanel
National Accelerator Laboratory
P.O. Box 500
Batavia, Illinois 60510

Aerospace Corporation
Attn: Dr. Thomas Taylor
P.O. Box 5866
San Bernardino, California 92408

Dr. A. L. Anderson
Applied Research Laboratory
University of Texas
P.O. Drawer 8029
Austin, Texas 78712

Dr. V. C. Anderson
Scripps Institution of Oceanography
University of California
La Jolla, California 92037

Applied Research Laboratory
Pennsylvania State University
Attn: W. Baker
H. M. Jensen
S. McDaniel
Dr. H. S. Piper
D. C. Stickler
P.O. Box 30
State College, Pennsylvania 16801

Capt. J. C. Bajus Code 03
Naval Electronic Systems Command Hdqs.
Department of the Navy
Washington, D.C. 20360

Dr. R. W. Bannister
Defense Scientific Establishment
HMNZ Dockyard, Devonport
Auckland 45400, New Zealand

Bell Telephone Laboratories
Attn: R. Hardin
R. Holford
T. E. Talpey
Whippany, New Jersey 07901

Dr. H. F. Bezdek
Office of Naval Research (480)
Department of the Navy
Arlington, Virginia 22217

Prof. Theodore G. Birdsall, Director
Cooley Electronics Laboratory
Cooley Bldg., North Campus
University of Michigan
Ann Arbor, Michigan 48105

Dr. Martin H. Bloom
Polytechnic Institute of Brooklyn
Route 110, Room 205
Farmingdale, New York 11735

Cmdr. A. G. Brookes, Jr.
Office of Naval Research (Code 102-OS)
Department of the Navy
Arlington, Virginia 22217

Brown University
Department of Mathematics
Attn: C. Dafermos
W. Strauss
Providence, Rhode Island 02912

Mr. D. G. Browning
New London Laboratory
Naval Underwater Systems Center
New London, Connecticut 06320

Mr. B. M. Buck
Polar Research Laboratory, Inc.
123 Santa Barbara St.
Santa Barbara, California 93101

California Institute of Technology
Attn: Dr. Milton Plesset
Dr. Toshi Kubota
1201 East California Blvd.
Pasadena, California 91109

Dr. Curtis G. Callan, Jr.
Department of Physics
Princeton University
Princeton, New Jersey 08540

Dr. G. F. Carrier
Harvard University
Pierce Hall
Cambridge, Massachusetts 02139

Catholic University
Attn: F. Andrews
H. Uberall
620 Michigan Ave., NE
Washington, D.C. 20017

Courant Institute
Attn: D. Ahluwalia
C. Aquista
J. Bazer
R. Burridge
J. Keller
C. Morawetz
G. Papanicolaou
P. Sulem
J. Weileman
251 Mercer St.
New York, New York 10012

Capt. C. G. Darrell
Director, Undersea Warfare Technology
Office of Naval Research (Code 412)
Arlington, Virginia 22217

Dr. Roger F. Dashen
Institute for Advanced Study
Princeton, New Jersey 08540

Defence Research Establishment
Atlantic
Attn: Mr. J. B. Franklin
Dr. R. S. Thomas
P.O. Box 1012
Dartmouth, Nova Scotia, Canada

Defence Research Establishment
Pacific
Department of National Defence
Attn: Dr. R. P. Chapman
Mr. J. M. Thorliefson
Forces Mail Office
Victoria, B.C., VOS 1BO, Canada

Defense Advanced Research Projects
Agency
Attn: Mr. Robert M. Chapman, TTO
Mr. Craig W. Hartsell, Jr., STO
Dr. George H. Heilmeier, Director
Dr. Richard F. Hoglund, TTO
Dr. Donald J. Looft, Dep. Director
Mr. Robert A. Moore, TTO
Dr. Stephen Zakanycz
1400 Wilson Boulevard
Arlington Virginia 22209

Prof. I. Dyer
MIT
Department of Ocean Engineering
Cambridge, Massachusetts 02139

Prof. Freeman J. Dyson
Institute for Advanced Study
Princeton, New Jersey 08540

Dr. Harlow Farmer
P.O. 1925 (Main Station)
Washington, D.C. 20013

Dr. F. Fisher
Scripps Institution of Oceanography
University of California, San Diego
La Jolla, California 92037

Dr. R. M. Fitzgerald
Naval Research Laboratory
Department of the Navy
Washington, D.C. 20375

Dr. Stanley M. Flatté
360 Moore St.
Santa Cruz, California 95064

Flow Research, Inc.
Attn: Dr. Denny R. S. Ko
Dr. Michael Y. H. Pao
1810 South Central Ave.
Suite 72
Kent, Washington 98031

General Research Corp.
Attn: Mr. P. Donohoe
1501 Wilson Blvd.
Suite 700
Arlington, Virginia 22209

George Washington University
Computer Science and E.E.
Attn: R. Lang
Washington, D.C. 20006

Dr. R. R. Goodman Code 8000
Associate Director of Research
Naval Research Laboratory
Department of the Navy
Washington, D.C. 20375

Mr. W. Griswold
U.S. Naval Ship Research and
Development Center
Annapolis, Maryland 21402

Mr. I. Hagan
Royal Australian Navy Research
Laboratory
New Beach Road
Edgecliff, NSW, Australia 2027

Mr. G. R. Hamilton, Director
Ocean Science and Technology Division
Office of Naval Research
Department of the Navy
Arlington, Virginia 22217

Dr. J. S. Hanna
Office of Naval Research (AESD)
Department of the Navy
Arlington, Virginia 22217

Hawaii Institute of Geophysics
University of Hawaii
Attn: Dr. W. E. Hardy
Mr. P. M. Volk
2525 Correa Rd.
Honolulu, Hawaii 96822

Dr. J. B. Hersey
Bldg. 58
Naval Research Laboratory
Washington, D.C. 20390

Dr. C. W. Horton, Sr.
Applied Research Laboratory
University of Texas
P.O. Drawer 8029
Austin, Texas 78712

Dr. Norden Hueng
Department of Geosciences
North Carolina State University
Raleigh, North Carolina 27607

Hydronautics, Inc.
Attn: Dr. O. M. Phillips
Dr. T. R. Sundaram
Dr. J. Wu
Pindell School Rd., Howard Co.
Laurel, Maryland 20810

Imperial College
Department of E.E.
Attn: R. Clarke
Exhibition Road
London SW7, England

Institute for Acoustical Research
University of Miami
Attn: Dr. J. G. Clark
Dr. Martin Kronengold, Director
615 SW Second Ave.
Miami, Florida 33130

Institute for Defense Analysis
Attn: Dr. Joel Bengston
Mr. J. C. Nolen
Dr. Philip A. Selwyn
400 Army-Navy Drive
Arlington, Virginia 22202

Frank Jablonski (OPNAV)
Room 4B489
The Pentagon
Washington, D.C. 20350

Capt. D. M. Jackson
Naval Electronic Systems
Command Hdqs.
PME-124
Washington, D.C. 20360

Johns Hopkins University
Applied Physics Laboratory
Attn: L. Cronvich
H. Gilreath
N. Nicholas
A. Stone
8621 Georgia Ave.
Silver Spring, Maryland 20910

Dr. I.S.F. Jones
Head, Ocean Science Group
Royal Australian Navy Research
Laboratory
New Beach Road
Edgecliff, NSW, Australia 2027

Lamont-Doherty Geological Observatory
Columbia University
Attn: Mr. J. I. Ewing
Dr. H. Kutshale
Palisades, New York 10964

Dr. Frank Lane
KLD Associates, Inc.
7 High St., Suite 204
Huntington, New York 11743

Dr. W. S. Lewellen
Aeronautical Research Associates
of Princeton, Inc.
50 Washington Rd.
Princeton, New Jersey 08540

Dr. Harold W. Lewis
Department of Physics
University of California
Santa Barbara, California 93106

Mr. P. H. Lindop
Admiralty Research Laboratory
Teddington, Middlesex
England

Dr. S. W. Marshall
Naval Research Laboratory
Department of the Navy
Washington, D.C. 20375

Massachusetts Institute of Technology
Department of Mechanical Engineering
Attn: Dr. Eric L. Mollo-Christenson
Cambridge, Massachusetts 02139

Massachusetts Institute of Technology
Lincoln Laboratory
Attn: Dr. Charles W. Rook
P.O. Box 73
Lexington, Massachusetts 02173

Prof. H. Medwin
Naval Postgraduate School
Department of Physics
Monterey, California 93940

Cmdr. R. Miller (OPNAV)
Room 5D572
The Pentagon
Washington, D.C. 20390

Dr. G. A. Morgan
Embassy of Australia
1601 Massachusetts Ave., NW
Washington, D.C. 20036

Dr. W. Moseley Code 8160
Naval Research Laboratory
Department of the Navy
Washington, D.C. 20375

Dr. Walter H. Munk
9530 La Jolla Shores Drive
La Jolla, California 92037

NATO
SACLANT ASW Research Center
Attn: Dr. Bruce Williams
Dr. D. Wood
Viale San Bartolomeo, 400
1-19026 La Spezia, Italy

Naval Air Development Center
Attn: C. Bartberger
E. P. Garabed Code 2052
Warminster, Pennsylvania 18974

Naval Air Systems Command
Main Navy Bldg.
Attn: I. H. Gatzke
Washington, D.C. 20360

Naval Oceanographic Office
Attn: Mr. W. H. Geddes
Dr. M. Schulkin
Suitland, Maryland 20373

Naval Ordnance Laboratory
White Oak
Attn: I. Blatstein
Ms. E. A. Christian
R. J. Urick
Silver Spring, Maryland 20910

Naval Research Laboratory
Attn: R. Baer
A. Berman
J. Cybulsky
J. Dugan
J. O. Elliot
B. Hurdle
F. Ingenito
Frank MacDonald
J. McCoy
S. Piacsek
K. G. Williams
4555 Overlook Ave., SW
Washington, D.C. 20390

Naval Scientific and Technical
Intelligence Center
Attn: Capt. J. P. Prisley
4301 Suitland Rd.
Washington, D.C. 20390

Naval Ship Systems Command
TRIDENT Project Officer
Washington, D.C. 20360

Naval Undersea Center
Attn: H. S. Aurand, Jr., Head,
Ocean Acoustics Division
Dr. H. Bucker
Dr. A. G. Fabula
E. Floyd
D. Gordon
H. Morris
J. Neubert
M. A. Pedersen
C. Ramstedt
D. White
San Diego, California 92132

Naval Undersea Systems Center
Attn: Dr. J. D'Albora
Newport, Rhode Island 02840

Naval Underwater Systems Center
New London Laboratory
Attn: D. Abraham
D. G. Browning
J. Cohen
H. Cox
R. Deavenport
F. Dinapoli
L. Einstein
A. Ellinthorpe
R. Elswick
H. Freese
O. D. Grace
J. Hassab
E. Jensen
W. Kanabis
A. Krulisch
R. Lauer
G. Leibiger
R. L. Martin
R. H. Mellen
J. Papadakis
W. I. Roderick
R. Saenger
P. Scully-Power
D. Shoening
L. Stallworth
W. A. Von Winkle
H. Weinberg
New London, Connecticut 06320

Dr. William A. Nierenberg
Scripps Institution of Oceanography
University of California
La Jolla, California 92037

ODDR&E
The Pentagon
Attn: G. Cann, Rm. 3D1048
Dr. D. R. Heebner, Rm 3E1040
N. F. Wikner, Rm 3E1087
Washington, D.C. 20301

Office of Naval Research
Attn: Dr. W. J. Condell
Mr. A. O. Sykes, Code 412
800 N. Quincy St.
Arlington, Virginia 22217

Office of Naval Research
Attn: D. Cacchione
495 Summer St.
Boston, Massachusetts 22210

Office of Naval Research
Acoustic Environmental Support
Detachment
Attn: R. Buchal
Dr. R. C. Cavanagh
A. Cecelski
S. Reed, Jr.
C. W. Spofford
Lcdr. B. T. Steele
Cdr. P. R. Tatro, Head
Arlington, Virginia 22217

Office of Naval Research
Department of the Navy
Attn: Cdr. J. Ballou
M. Cooper
R. Cooper
J. Witting
Washington, D.C. 20360

Physical Dynamics, Inc.
Attn: Dr. Alex Thomson
Dr. Bruce West
P.O. Box 1069
Berkeley, California 94704

Capt. Daniel Piraino (NSP)
SP202
Department of the Navy
Washington, D.C. 20390

Polytechnic Institute of New York
Department of Mathematics
Attn: H. Hockstadt
333 Jay St.
Brooklyn, New York 11201

James H. Probus (OASN)
Room 4E741
The Pentagon
Washington, D.C. 20350

R&D Associates
Attn: Dr. F. L. Fernandez
Dr. D. Holliday
Dr. M. Milder
P.O. Box 3580
Santa Monica, California 90403

Dr. Gordon Raisbeck
Arthur D. Kittle, Inc.
Cambridge, Massachusetts 02140

Rensselaer Polytechnic Institute
Department of Mathematics
Attn: M. Jacobson
Troy, New York 12181

Riverside Research Institute
Attn: Dr. Marvin King
80 West End Ave.
New York, New York 10023

Mr. D. A. Rogers (NSP)
SP2018
Department of the Navy
Washington, D.C. 20390

Mr. Benjamin Rosenberg (OPNAV)
Room 4B513
The Pentagon
Washington, D.C. 20350

Rosentiel School of Marine and
Atmospheric Science
University of Miami
Attn: Dr. S. C. Daubin
Dr. H. DeFarrari
Miami, Florida 33149

Dr. Donald Ross
Tetra Tech, Inc.
3559 Kenyon Street
San Diego, California 92110

Science Application, Inc.
Attn: H. Wilson
P.O. Box 351
La Jolla, California 92037

Mr. Carey Smith
Naval Sea Systems Command Hdqs.
Code 06H1
Department of the Navy
Washington, D.C. 20360

Stanford Research Institute
Attn: N. Cianos, 44
H. Guthart, 404B
R. C. Honey, 406A
K. Krishnan, K1068
333 Ravenswood Ave.
Menlo Park, California 94025

TRW Systems Group
Attn: E. Baum
J. Chang
One Space Park
Redondo Beach, California 90278

Dr. F. Tappert
Courant Institute
251 Mercer St.
New York, New York 10012

Dr. C. M. Tchen
1380 Riverside Drive
New York, New York 10033

University of California
Lawrence Radiation Laboratory
Attn: Dr. Harold P. Smith
Dr. M. Wirth
P.O. Box 808
Livermore, California 94550

University of California, San Diego
Attn: Dr. C. Cox
Dr. R. Davis
Dr. C. Gibson
Dr. J. Miles
P.O. Box 119
La Jolla, California 92038

University of California
Scripps Institution of Oceanography
Marine Physical Laboratory
Attn: Dr. T. Foster
Dr. G. B. Morris
Dr. F. Spiess
San Diego, California 92152

University of Rhode Island
Attn: G. Ladas E. Roxin
L. LeBlanc R. Suryanarayan
F. Middleton G. Verma
A. Poularicas
Kingston, Rhode Island 02881

Dr. Roberto Vaglio-Laurin
Advanced Technology Laboratories, Inc.
400 Jericho Turnpike
Jericho, New York 11753

Virginia Polytechnic Institute
State University
Attn: I. Tolstoy
W. Kohler
Blacksbury, Virginia 24061

Cdr. Don Walsh (OASN/R&D)
Room 4E741
The Pentagon
Washington, D.C. 20350

Dr. Kenneth M. Watson
Lawrence Berkeley Laboratory
University of California
Berkeley, California 94720

Wayne State University
Department of Mathematics
Attn: P. Chow
Detroit, Michigan 46202

Dr. M. S. Weinstein
Underwater Systems, Inc.
8121 Georgia Ave., Suite 700
Silver Spring, Maryland 20910

Western Electric Co.
Bell Telephone Laboratories
Attn: Dr. E. Y. Harper
Dr. F. Labianca
Whippany, New Jersey 07981

M. Wilson
Naval Ship Research and Development
Center
Washington, D.C. 20007

Woods Hole Oceanographic Institution
Attn: Dr. E. E. Hays
Dr. R. Porter
Dr. R. Spindel
Mr. W. A. Watkins
Woods Hole, Massachusetts 02543

Dr. J. L. Worzel
Marine Science Institute
Geophysics Laboratory
700 Thestrand
Galveston, Texas 77550

Dr. D. V. Wyllie
Weapons Research Establishment
Box 2151, G.P.O.
Adelaide, South Australia 5001

Dr. H. Yura
Aerospace Corporation
P.O. Box 92956
Los Angeles, California 90009

Dr. Fredrik Zachariasen
#452-48
Department of Physics
California Institute of Technology
Pasadena, California 91109